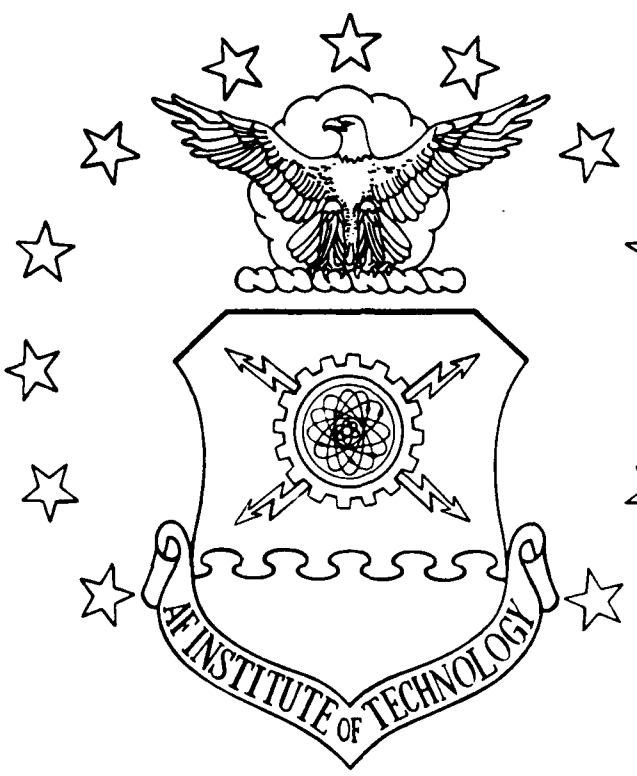

FREQUENCY-DEPENDENT MATERIAL DAMPING USING AUGMENTING THERMODYNAMIC FIELDS (ATF) WITH FRACTIONAL TIME DERIVATIVES

David S. Hansen
First Lieutenant, USAF

AFIT/GAE/ENY/90S-1

DEPARTMENT OF THE AIR FORCE
AIR UNIVERSITY
AIR FORCE INSTITUTE OF TECHNOLOGY

Wright-Patterson Air Force Base, Ohio

(1)

FREQUENCY-DEPENDENT MATERIAL DAMPING USING AUGMENTING THERMODYNAMIC FIELDS (ATF) WITH FRACTIONAL TIME DERIVATIVES

David S. Hansen
First Lieutenant, USAF

AFIT/GAE/ENY/90S-1

AFIT/GAE/ENY/90S-1

FREQUENCY-DEPENDENT MATERIAL DAMPING USING AUGMENTING THERMODYNAMIC FIELDS (ATF) WITH FRACTIONAL TIME DERIVATIVES

THESIS

Presented to the Faculty of the School of Engineering
of the Air Force Institute of Technology
Air University
In Partial Fulfillment of the
Requirements for the Degree of
Master of Science in Aeronautical Engineering

David S. Hansen, B.S.
First Lieutenant, USAF

September 1990

Preface

The purpose of this study was to gain a better understanding of the modeling of material damping. With increased operations in a non-atmosphere environment such as space, the need exists for better and more accurate models of material damping, models that include the fundamental dependence of material damping on frequency, so that systems designed for these environments will be the best possible.

In performing the research behind this thesis I constantly relied on a man who, in my mind, easily fits in the genius category. Dr. Torvik, I will always be indebted for your help, your gentle prodding, your knowledge that kept me from floundering in deep waters, and your friendship. I also wish to thank Lt. Col. Bagley, a man I greatly admire, for his enthusiasm and overwhelming desire for my success, and for his work that helped this effort. And to Lt. Col. King for his sage words of advice, and help as a committee member.

But perhaps I owe the most to my helpmeet and eternal companion. Thanks, Lisa, for loving me and pushing me through the trying times we had in school. This degree is truly yours, for you inspire me to be better. Finally, to the rug rats who bring much joy in my life. Nathan, Ryan, and Megan...warm up the Nintendo, get the matchbox cars out, practice up on patty-cake --- Daddy's coming home!

David S. Hansen

Table of Contents

List of Figures

List of Symbols

A - affinity

a_k - acceleration

a_n, b_n - viscoelastic model parameters

b - material parameter of viscoelastic model

B - material parameter, proportionality constant of the ATF equilibrium equation

c - damping coefficient (dashpot coefficient)

c_c - critical damping

c_{eq} - equivalent damping coefficient

c_p - specific heat at constant pressure, per unit volume

c_v - specific heat at constant volume, per unit volume

D - dissipation energy

D_{**} - denominator of complex modulus, loss factor, and damping ratio

E - Young's modulus of elasticity

E^* - complex modulus

E_A - adiabatic modulus of elasticity

E_g - glassy modulus of elasticity, $E_g = E_1/b$

E_o - rubbery modulus of elasticity

E_T - isothermal modulus of elasticity

E_1 - material constant of viscoelastic model

F^T - Fourier transform

$F(t)$ - forcing function

f - Helmholtz free energy

f_k - body forces

i - complex number = $(-1)^{1/2}$

K - spring constant

k - spatial frequency (wave number)

M - mass

m, n - integers used in integer order derivatives

N_{**} - numerator term in complex modulus, loss factor, and damping ratio

Q - resonant amplification factor

q, r, s - rational numbers used in fractional order derivatives

T - temperature change

$\bar{T}$ - Fourier transform of temperature change

T_o - initial temperature

t_{lk} - stress tensor

u - displacement

U_s - strain energy

U, $\bar{X}$ - Fourier transform of the displacement, u, x

x - $q\pi/2$

y - $r\pi/2$

Z - Fourier transform of the augmenting thermodynamic field,

z - $(q + r)\pi/2$

α_1, α_2 - material parameter, relation of affinity to the augmenting thermodynamic field

α_3 - coupling between two ATFs

α_T - coefficient of thermal expansion

γ - complex stiffness parameter

γ - $= 1 - \alpha_3{}^2/\alpha^1\alpha^2$, ATF model parameter

δ - material parameter, coupling parameter of u and ξ

δ_{ij} - Kronecker delta

δ_D - logarithmic decrement

ϵ - strain

ζ - damping ratio

η - loss factor

κ - thermal conductivity

λ, μ - Lame's constants

μ_N - Newtonian viscocity coefficient

ξ - augmenting thermodynamic field

$\bar{\xi}$ - equilibrium value of ATF

ρ - mass density

σ - stress

τ - integration parameter

ν - Poisson's ratio

ω - frequency

ω_n - undamped natural frequency

Γ - gamma function

Δ_1, Δ_2 - ATF model parameter = $\delta^2/E\alpha$

Δ_3 - ATF model material coupling parameter = $\delta_1\delta_2\alpha_3/E\alpha_1\alpha_2$

ψ - damping capacity

Abstract

The purpose of this study is the development of a model using the concept of augmenting thermodynamic fields (ATF), wherein the equations of thermodynamic equilibirum are allowed to have derivatives of fractional order. This effort seeks to expand the applicabilty of the augmenting thermodynamic field model, in which augmenting thermodynamic fields interact with the mechanical displacement field. The ATF model was introduced by Lesieutre in a dissertation submitted to the University of California, Los Angeles.

Current methods of analyzing material damping analysis, not being physically motivated, cannot predict well the dependency of damping on frequency. Two newer methods, capable of predicting this frequency dependence, are discussed. They include the ATF model of Lesieutre, and the 4-parameter model, which allows fractional derivatives in the description of viscoelastic materials, introduced by Bagley and Torvik of the Air Force Institute of Technology.

This research effort applies the fractional derivative concept of Bagley and Torvik's model to the model of Lesieutre. Capitalizing on the previously made observation that the use of fractional derivatives in material models enables the description of material damping over a much broader frequency range, coupled material constitutive

relations are developed using the concept of augmenting thermodynamic fields, with non-integer differentials allowed in the resulting partial differential equations.

The complex modulus that results from solution of these partial differential equations is compared to the complex moduli of thermoelasticity, integer-order viscoelasticity, and viscoelasticity with fractional derivatives (the 4-parameter model) for the case of a uniaxial rod. In each case, the fractional-order ATF model reduced to the respective model, and, therefore, accurately describes the damping mechanism resulting from each of these models.

The fractional-order ATF model can be used to accurately describe material damping caused both by thermoelasticity and by viscoelasticity over a broad frequency range.

FREQUENCY-DEPENDENT MATERIAL DAMPING USING AUGMENTING THERMODYNAMIC FIELDS (ATF) WITH FRACTIONAL TIME DERIVATIVES

I. Introduction

Damping in Structures

The free vibration of any system will eventually die out due to some form of energy dissipation. This energy dissipation is commonly referred to as damping. Damping in a structure is a result of energy dissipation mechanisms which can be divided into three broad categories (Lesieutre, 1989:4): (1) internal or material damping caused by the deformation of the material; (2) joint impact or friction damping, caused by the dissimilar deformations at structural component interfaces; and (3) energy dissipation caused by the structure's interaction with non-strucutral components or the surrounding environment.

An illustration of each of these types of damping may be demonstrated through an example of a car driving down the highway, with the car being the system under consideration. Energy is dissipated through the movement and flexure of the automobile components; this is material damping. Gears, the engine, and interaction of the assembled components of the car, all represent joint or friction damping. Energy loss

caused by air drag and the interaction of the tires with the highway are examples of the third type of damping of structures.

For most systems in use in the atmosphere, the last two types of energy dissipation mechanisms will dominate. In space, however, the interaction with the environment practically disappears, and the requirements for highly precise instruments and low vibration levels will greatly reduce the loss mechanism found in joint and friction damping. Thus, material damping becomes much more important, and an accurate model of this material damping is needed.

Material damping generally depends on many factors including frequency, temperature, geometry of the structure, stress (or strain) history, and deformations. The interaction of these factors leads to a complex mathematical problem. Zener, in his discussion of relaxation and internal friction (material damping), plots the internal friction versus the logarithm of time, and calls it the relaxtion spectrum (Zener, 1948:Frontispiece). Such a figure, as replicated in figure 1, is believed to be typical of the frequency dependence of material damping. Zener calculated the internal friction caused by various material interactions such as grain boundaries or transverse thermal currents, and then linearly superimposed the results to produce the graph of figure 1. Many of the damping models

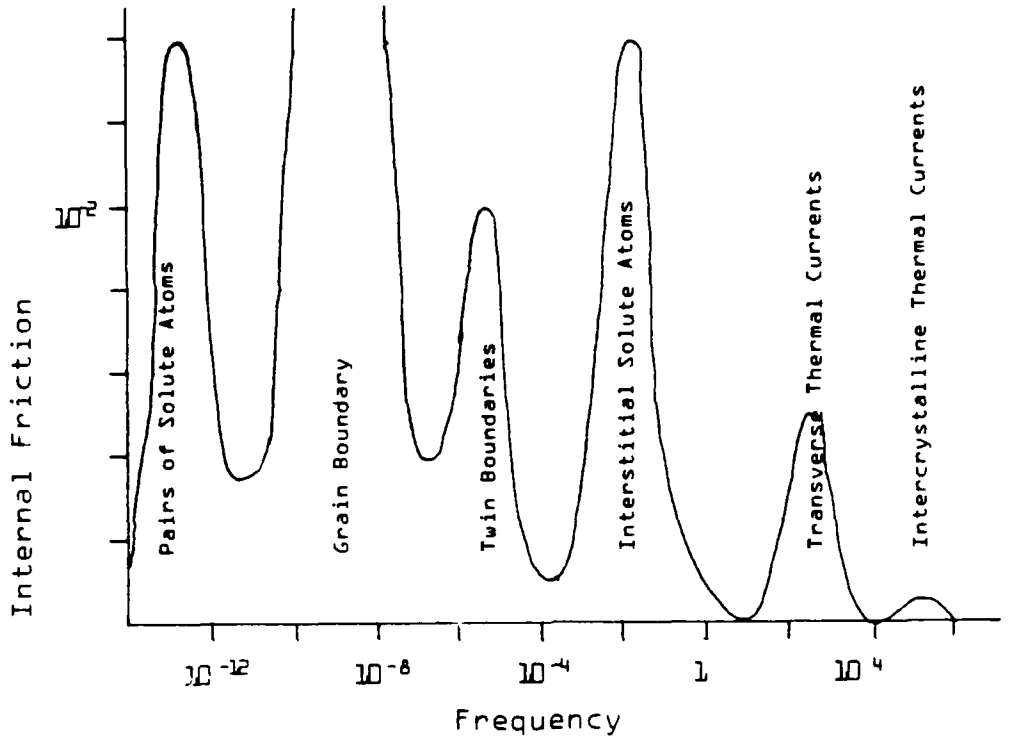

Figure 1. Internal Friction (damping) Versus Frequency

in use today are unable to reproduce this frequency dependence and are therefore inadequate in not being fully descriptive of the actual material behavior.

Damping Conventions

The world of damping is not a new one, although a new emphasis has been placed on it due to expanded operations in environments (space) where damping becomes very important. It is important, therefore, to review the nomenclature, notation, and models that have become standard in structural dynamics study.

Damping Nomenclature. The spring-mass-dashpot system of figure 2 is the simplest and most commonly used model of

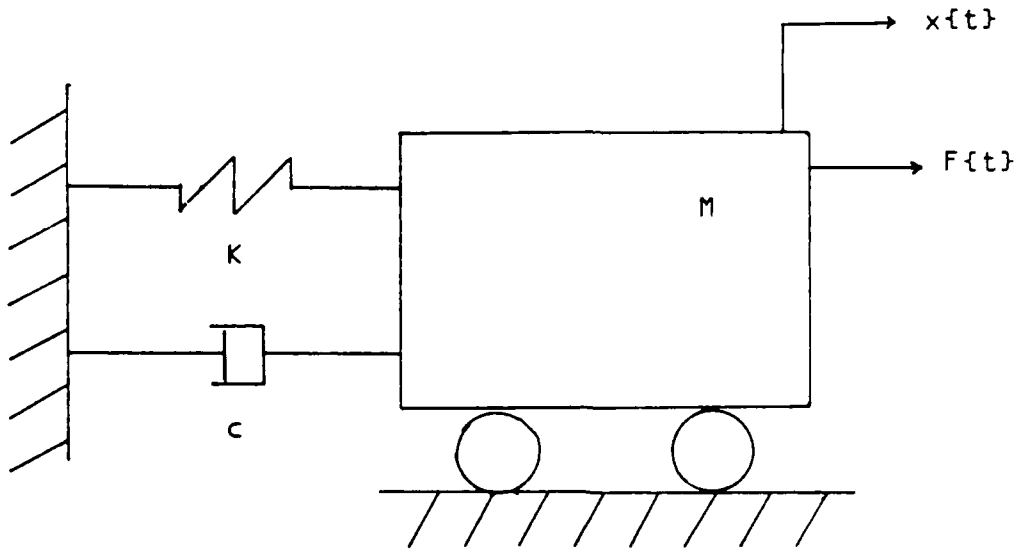

Figure 2. Spring-mass-dashpot System

systems with damping. It is also known as the viscous damping model, and results in the equations of motion

$$M\ddot{x} + c\dot{x} + Kx = F(t) \qquad (1)$$

for the single degree-of-freedom system with mass M, stiffness K, dashpot coefficient c, and force F(t). Several system parameters come from this equation. They are listed and briefly described below:

ω_n - Undamped Natural Frequency. Defined as $\omega_n=(K/M)^{1/2}$, and also known as the natural frequency, this is the frequency at which the system would vibrate if there were no damping and no forcing function.

c_c - Critical Damping. Defined as $c_c=2(KM)^{1/2}$, this is the dashpot coefficient which would be required for a non-oscillatory response of the free system (F(t) = 0).

ζ - Damping Ratio. This is the ratio of the actual dashpot coefficent c to the critical damping c_c. It can be shown that the time response of a freely vibrating spring-mass-dashpot system displays a decay characterized by $e^{-\zeta \omega_n t}$.

Damping Measures. Several measures of damping are currently in use. Some are listed below, together with their definitions.

Q - Resonant Amplification Factor. The ratio of the amplitude of the internal force to that of the external force. The compliance is equal to the reciprocal of this. At resonance, $\omega = \omega_n$, and Q is equal to one over twice the damping ratio.

δ_D - Logarithmic Decrement. This is equal to the natural logarithm of the ratio of the amplitudes of two consecutive displacements x_1 and x_2, one cycle apart, or the logarithm of the ratio of the amplitudes of two displacements x_1 and x_N, N-cycles apart divided by the number of cycles:

$$\delta_D = (1/N) \ln(x_1/x_N) \qquad (2)$$

This is particularly useful in experimentally finding the damping of a system. For small damping, δ is a small quantity, and $\zeta = \delta/2$.

D - Dissipation. The dissipation is equal to the amount of energy dissipated in one oscillatory cycle:

$$D = \int_0^{2\pi/\omega} \sigma \dot{\epsilon} \, dt \qquad (3)$$

If divided by the peak value of strain energy stored within the cycle, U_s, this results in the Damping Capacity, ψ, commonly used by materials scientists. The Damping Capacity is equal to 4π times the damping ratio.

η - Loss Factor. The ratio of the energy dissipated per radian of vibration to the maximum energy stored is equal to the loss factor. It is also defined as the ratio of a material's loss modulus to its storage modulus. With respect to the complex modulus E^*, it is the ratio of the imaginary and real parts:

$$\eta = Im(E^*)/Re(E^*) \tag{4}$$

A comparison of these damping measures to the damping ratio results in the following, for small damping:

$$\zeta = 1/2Q = \delta_D/2\pi = \psi/4\pi = \eta/2 \tag{5}$$

Damping Mechanism Models

The linear matrix differential equation used most commonly in structural dynamics models is

$$[M]\{\ddot{x}\} + [c]\{\dot{x}\} + [K]\{x\} = \{F\}. \tag{6}$$

The mass matrix [M] is positive, definite, and the stiffness matrix [K] is positive, semi-definite. Both are symmetric, and are easily found from the mechanics of the problem, as is the force vector {F}. The damping matrix [c], although positive semi-definite and symmetric, cannot be easily derived, except in trivial cases.

There are several methods of incorporating damping into structural models. These include, but are not limited to,

viscous damping, viscoelastic damping, complex modulus, and structural damping. Each will be discussed, in scalar form, briefly below.

Viscous Damping. Viscous damping assumes that damping forces are proportional to the time rate of change of strain, and thus, displacement. This results in the equation of motion given by equation (1). Rewriting this equation using the constants defined above and setting F(t)=0 gives

$$\ddot{x} + 2\zeta\omega_n \dot{x} + \omega_n^2 x = 0 \qquad (7)$$

It will later be shown that the dissipation of a Kelvin solid increases monotonically with frequency. Most materials do not behave in such a manner, except over small frequency ranges, and this model, therefore, although mathematically simple, is not very useful.

Viscoelastic Damping. The stress-strain relationship of a viscoelastic material may be described by the generalized linear constitutive equation as

$$\sum_{m=1}^{M} b_m \frac{d^m\sigma}{dt^m} = \sum_{n=1}^{N} a_n \frac{d^n\epsilon}{dt^n} \qquad (8)$$

In the simplest case, this is equivalent to viscous damping, i.e.,

$$\sigma = a_o\epsilon + a_1 d\epsilon/dt \qquad (9)$$

since b_o may be set to unity without loss of generality. In this case, a_o represents the elastic modulus ,E, and a_1 represents the Newtonian viscosity coefficient, μ_N.

The description of more complex behavior is accomplished with the inclusion of more terms, in turn allowing a more accurate model over a broader frequency range. This, however, quickly becomes tedious, if not impossible mathematically.

Complex Modulus. Taking the Fourier Transform

$$F^T[X(t)] = \int_{-\infty}^{\infty} e^{-i\omega t} X(t)dt \qquad (10)$$

of equation (9), where temporal derivatives introduce $i\omega$, gives

$$\bar{\sigma}(\omega) = E\bar{\epsilon}(\omega) + i\mu_N\omega\bar{\epsilon}(\omega) \qquad (11)$$

Dividing both sides by $\bar{\epsilon}$ gives

$$\bar{\sigma}/\bar{\epsilon} = E + i\mu_N\omega \qquad (12)$$

Equation (12) suggests the possibility of a complex modulus, $E^* = E_1 + iE_2$, which may be used in many damping models. If $\epsilon = Re[\epsilon_o \exp(i\omega t)] = \epsilon_o \cos(\omega t)$ for real ϵ_o, then

$$\sigma = Re[E^*\epsilon_o e^{i\omega t}]$$

$$= \epsilon_o[E_1\cos(\omega t) - E_2\sin(\omega t)] \qquad (13)$$

Recall that the energy dissipated per cycle, for real ϵ_o, is given by

$$D = \int_0^{2\omega/} \sigma\,\dot{\epsilon}\,dt$$

$$= \int_0^{2\omega/} \epsilon_o[E_1\cos(\omega t) - E_2\sin(\omega t)](-\omega)\epsilon_o\sin(\omega t)dt$$

$$= E_2\epsilon_o^2\pi \qquad (14)$$

Note that D is now independent of frequency. The peak stored energy, U_s, is given by

$$U_s = 1/2\ E_1 \epsilon_o^2 \tag{15}$$

Therefore, the damping capacity is equal to

$$D/U_s = 2\pi E_2/E_1 \tag{16}$$

and the damping ratio is

$$\zeta = D/(4\pi U_s) = 1/2\ E_2/E_1. \tag{17}$$

Structural Damping. Structural damping does not depend on the time rate of strain, as in viscous damping, but depends on the amplitude of oscillation over a wide frequency range. So, for systems under harmonic excitation, the "c" or damping of equation (1) may be treated as inversely proportional to the driving frequency (Meirovitch, 1986:71-73;1967:400-403):

$$c_{eq} = \alpha/(\pi\omega) \tag{18}$$

Equation (1) may then be rewritten as

$$M\ddot{x} + [\alpha/(\pi\omega)]\dot{x} + Kx = F(t) \tag{19}$$

which is not really an equation since it mixes time derivatives and frequencies. The consequence is that this approach is only applicable in modeling constant-amplitude forced vibrations at single frequencies. Taking the Fourier transform of x(t) gives $i\omega\bar{X}$, where $\bar{X}$ is the Fourier transform of x(t), thus motivating the rewriting of equation (19) as the pseudo-equation

$$M\ddot{x} + K(1 + i\gamma)x = F(t) \tag{20}$$

where

$$\gamma = \alpha/(\pi K) \tag{21}$$

which is equivalent to the loss factor. The quantity $K(1 + i\gamma)$ is sometimes called the complex stiffness or complex damping model.

Augmenting Thermodynamic Field model with Fractional Derivatives. This research effort applies concepts of recent research undertaken by Torvik and Bagley of the Air Force Institute of Technology, Wright Patterson Air Force Base, to the research efforts of Lesieutre, formerly of the University of California, Los Angeles. Bagley and Torvik have described, in a series of papers (Bagley and Torvik, 1986; 1983; Torvik and Bagley, 1987; 1984), the application of material models involving the fractional derivative to problems in vibration. Lesieutre in his doctoral dissertation (Lesieutre, 1989) introduced the notion of augmenting thermodynamic fields to describe a new method of modeling frequency-dependent material damping in structural damping analysis. This effort will apply fractional derivatives to the augmenting thermodynamic field model in an effort to expand the applicability of that model.

The utility of the ATF model with fractional derivatives will be demonstrated through comparison of the model with other material damping models including thermoelasticity, viscoelasticity, and viscoelasticity with fractional derivatives. It will be seen that the ATF model with fractional derivatives can be reduced to these models, and is, therefore, a more powerful model for use in material damping study.

II. Augmenting Thermodynamic Fields

Noting the physical significance of the internal state variables of materials science, Lesieutre (Lesieutre, 1989) introduced augmenting thermodynamic fields to interact with the mechanical displacement field of continuum dynamics. He then used nonequilibrium, irreversible thermodynamics to develop coupled constitutive and partial differential equations. His approach will be reviewed here as a basis for the work of this effort.

Anelasticity (Nowick and Berry, 1972:1-5). Nowick and Berry intoduce anelastic behavior formally by first considering an ideal elastic material, for which the relation of stress to strain is defined by Hooke's law $\sigma = E\epsilon$, where E is called the modulus of elasticity. For this material, three conditions result. They are: (1) the applied stress produces a unique strain response through an equilibrium relationship, i.e., there is complete recoverability, (2) the equilibrium relationship produces an instantaneous response, and (3) the response is linear. By lifting the instantaneity condition, the type of behavior known as anelasticity is produced. With an anelastic material, a time dependent nonelastic response will occur in addition to the instantaneous elastic reaction.

All materials that qualify as thermodynamic solids satisfy the first condition above, since these solids can continuously assume unique equilibrium states in response to

small changes in some external variable such as stress or temperature. Relaxation is the self-adjustment with time of a thermodynamic system toward a new equilibrium values as a result of a change in some external variable (Nowick and Berry, 1972:4). Anelastic relaxation is the tendency of a thermodynamic system to evolve towards an equilibrium state when that state depends on an external mechanical value such as stress or strain.

Nowick and Berry summarize anelastic relaxation as the thermodynamic phenomenon which results from the changing of internal variables which couple stress and strain to new equilbrium values through such processes as kinetic diffusion (Nowick and Berry, 1972:5). Material damping is a direct result of such anelastic relaxation processes in real materials.

When the nature of the associated thermodynamic relaxation processes is considered, two classes of material damping mechanisms can be defined. They are damping as a result of system non-uniformity and damping as a result of a local departure from thermodynamic equilibrium (Lesieutre, 1989:23-26).

System Non-Uniformity. Thermoelasticity is a well-understood example of this type of damping mechanism. Torvik reviews this mechanism, stating that thermoelastic damping is a result of the coupling created when a thermal expansion term appears in the equation of state of a

material, as well as in the energy equation which describes the process (Torvik, 1989:2).

Consider an axial rod subjected to longitudinal elastic waves. During a cycle, one-half each wavelength of the rod undergoes an expansion with an accompanying increase in strain, and thus, an increase in volume. To satisfy the energy balance, temperature of this half of the rod must decrease. In an opposite sense, the temperature of the other half of the rod is increasing, due to the decrease in volume (compression) and strain of that half of the rod. The end result is a flow of heat by conduction along the longitudinal axis, causing temperature changes with time along the rod. These changes couple into the strain of the constituitive equation causing material damping, although, as was noted in Torvik's paper, this damping is small.

Local Departure from Thermodynamic Equilibrium (Lesieutre, 1989:24). Also known as microstructural damping, this damping is a result of the coupling of stress and strain with characteristics of real materials other than temperature. Material damping is affected by thermodynamic relaxations due to point defects, dislocations, or grain boundaries, which are thermally-activated, and are sensitive to the composition and microstructure of the material. These are all internal variables, evolving jointly with stress and strain, which motivated the introduction of augmenting thermodynamic fields (ATF) by Lesieutre. These

ATFs are to interact with the usual mechanical displacement field.

Irreversible Thermodynamics. The point defects of microstructural damping are thermally activated, leading one to the conclusion that material damping is fundamentally a thermodynamic phenomenon. Kovalenko states that the irreversible thermoelastic deformation of a body is a non-equilibrium process, with the irreversiblity being due to the temperature gradient (Kovalenko, 1969:7). A process associated with an increase in the entropy, with all real processes falling within this category, is said to be irreversible. This increase in entropy provides a quantitative measure of the irreversiblity of the process (Callen, 1960:63-65).

In irreversible thermodynamics the entropy balance equation plays a central role (Lesieutre, 1989:25-27). The rate of local entropy production equals the entropy leaving the region, plus the rate of entropy produced within the region (Callen, 1960:284-288). In others words, entropy of a volume element changes with time due to (1) entropy flow into the volume element, and (2) entropy created due to the irreversible processes inside the element. The entropy created, or the rate of production of entropy, is the sum of products of each flux with its associated affinity. Fluxes characterize some irreversible relaxation process, such as in a heat flux. The affinity can be thought of as the

generalized force which drives the irreversible process toward the equilibrium state.

Axial Rod With One Augmenting Thermodynamic Field (ATF) (Lesieutre, 1989:29-41). Lesieutre begins by considering the case of one-dimensional motion, corresponding to longitudinal vibration of a slender rod . Displacement along the rod is denoted by $u = u(x,t)$, mass density, which is uniform, by ρ, and the unrelaxed modulus of elasticity by E. He then introduces a single augmenting thermodynamic field (ATF), $\xi = \xi(x,t)$. The stress field, σ, is thermodynamically conjugate to the strain, ϵ, as is the affinity field, A, to the ATF, ξ. From irreversible thermodynamics, the affinity can be interpreted as the generalized force which drives ξ to equilibrium. The strength of the coupling of the two dependent fields, u and ξ, is described by the material property δ. If there were no coupling, the stress would be related to strain by Hooke's law. Analogously, the material property α relates changes in A to those in ξ.

Helmholtz Free Energy. Spanner states that, to have spontaneity of a process under isothermal conditions, the process must involve a decrease in free energy (Spanner, 1964:Ch 7). The Helmholtz free energy is used when no external volume work occurs as the process takes place.

The free energy of a system is not a part of its total energy. In truth, it is not simply an energy at all, but

represents the potentiality of the system doing work under the condition that the system is supplied with all the heating or cooling it requires to keep a constant temperature. When the system actually does work, it is at the expense of its free energy, with part of that work done out of its own resources, and part out of the heat energy supplied to it from its surroundings, resulting in an increase in system entropy (Spanner, 1964:91). Callen states that conditions are such in many processes that the ambient atmosphere acts as a heat reservoir to maintain the temperature constant (Callen, 1960:107). It is for these processes that the Helmholtz potential representation is well suited.

The state of system equilibrium is determined in an isothermal system by the condition of minimum free energy, ∂f. Here, ∂f represents the available useful work, other than pressure-volume work, at constant temperature and volume. If ∂f is negative the system will do work spontaneously. Processes for which this is the case are natural processes in the sense that work is done by the system in an effort to approach equilibrium (Penner, 1968:71).

The Helmholtz free energy density, f, being a thermodynamic potential appropriate for use when strain is an independent variable (Lesieutre, 1989:31), can be used to

derive the constitutive equations:

$$f = 1/2E\epsilon^2 - \delta\epsilon\xi + 1/2\alpha\xi^2 \tag{22}$$

Material Constitutive Equations. The constitutive equations are then found from the thermodynamic relations (Spanner, 1964:162)

$$\sigma = \partial f/\partial\epsilon \quad , \quad A = -\partial f/\partial\xi \tag{23}$$

which result in

$$\sigma = E\epsilon - \delta\xi \tag{24}$$

$$A = \delta\epsilon - \alpha\xi \tag{25}$$

In classical irreversible thermodynamics, it is assumed that the time rate of change of ξ is proportional to A, the affinity or thermodynamic force. For the quadratic dependence of equation (22) it is proportional to its deviation from an equilibrium value, $\bar{\xi}$, with the proportionality constant, B, being a material property different for any distinct dissipative mechanism:

$$\dot{\xi} = -B(\xi - \bar{\xi}) \tag{26}$$

where the dot $(\cdot)$ denotes temporal derivatives.

The value of $\bar{\xi}$ is the value of ξ at equilibrium, or when the affinity, the "generalized force" which drives ξ to equilibrium, is zero. Setting equation (25) to zero and solving for ξ gives

$$\bar{\xi} = \delta\epsilon/\alpha \tag{27}$$

which in turn can be substituted into equation (26) to give

$$\dot{\xi} = -B(\xi - \delta\epsilon/\alpha) \tag{28}$$

Cauchy's first law is invoked in order to insure conservation of linear momentum. In general

$$\underset{\sim}{t}_{lk,l} + \rho(\underset{\sim}{f}_k - \underset{\sim}{a}_k) = 0 \qquad (29)$$

where $\underset{\sim}{f}_k$ and $\underset{\sim}{a}_k$ are components of the body force and acceleration, repectively. For the case of axial motion of a one-dimensional bar, and neglecting body forces, this reduces to

$$\partial\sigma/\partial x - \rho a = \partial\sigma/\partial x - \rho\ddot{u} = 0 \qquad (30)$$

where the dot denotes temporal derivatives.

Recall that $\epsilon(x,t) = \partial u(x,t)/\partial x = u'$, where the prime denotes spatial derivatives. Using this, substituting equation (24) into equation (30), and rearranging terms gives, together with equation (28), a set of two coupled partial differential equations in u and ξ:

$$\begin{aligned} \rho\ddot{u} - Eu'' &= -\delta\xi' \\ \dot{\xi} + B\xi &= (B\delta/\alpha)u' \end{aligned} \qquad (31)$$

Lesieutre uses the principles of nonequilibrium irreversible thermodynamics to determine the conditions under which a given problem involving these equations is well-posed (Lesieutre, 1989:32-34). These conditions are

$$\rho > 0, \quad E > 0, \text{ and } \alpha > (\delta^2/E) > 0 \qquad (32)$$

conditions easily satisfied in practice.

Fourier Analysis. The set of equations (31) is a set of linear partial differential equations, and, as such, Fourier analysis may be used for their solution, especially since the frequency-dependence of the damping is of primary

interest. Consider a plane wave traveling in the negative x-direction with temporal frequency ω and spatial frequency (wave number) k according to $e^{i(kx+\omega t)}$. The Fourier transform of spatial derivatives will then introduce ik, and the transform of time derivatives will introduce $i\omega$, boundary conditions not being considered. Equation (31) yields

$$(-\rho\omega^2 + k^2E)U + ik\delta Z = 0 \tag{33}$$

$$(Bik\delta/\alpha)U - (B + i\omega)Z = 0 \tag{34}$$

where U and Z are the Fourier transforms of u(x) and $\xi(x)$, respectively.

Damping Ratio. Solving equation (34) for Z, and substituting into equation (33) gives, after algebraic manipulation

$$\frac{\rho\omega^2}{k^2} = E\left[\frac{1 - \Delta + i(\omega/B)}{1 + i(\omega/B)}\right] \tag{35}$$

where

$$\Delta = \delta^2/E\alpha \tag{36}$$

The term inside the [ ] brackets can be interpreted as a complex modulus, $E^*(\omega)$, which after further manipulation becomes

$$E^*(\omega) = E\left[\frac{1 - \Delta + (\omega/B)^2 + i(\Delta\omega/B)}{1 + (\omega/B)^2}\right] = 0 \tag{37}$$

and the loss factor, η, is found by

$$\eta = Im[E^*(\omega)]/Re[E^*(\omega)] \tag{38}$$

or, from equation (37)

$$\eta = \Delta(\omega/B)/[1 - \Delta + (\omega/B)^2] \quad (39)$$

If small damping is assumed, the damping ratio equals half of the loss factor (equation (5)):

$$\zeta = \Delta(\omega/B)/\{2[1 - \Delta + (\omega/B)^2]\} \quad (40)$$

For small damping the damping ratio is small, and the numerator of equation (40) must be small in comparison to its denominator. This being the case, Δ can be assumed small, and can be cancelled from the denominator, leaving the following equation for the damping ratio:

$$\zeta = (\delta^2/4E\alpha)(2\omega/B)/[1+(\omega/B)^2] \quad (41)$$

Figure 3 is a plot of the loss factor versus frequency for material property values that correspond roughly to aluminum (Lesieutre, 1989:48):

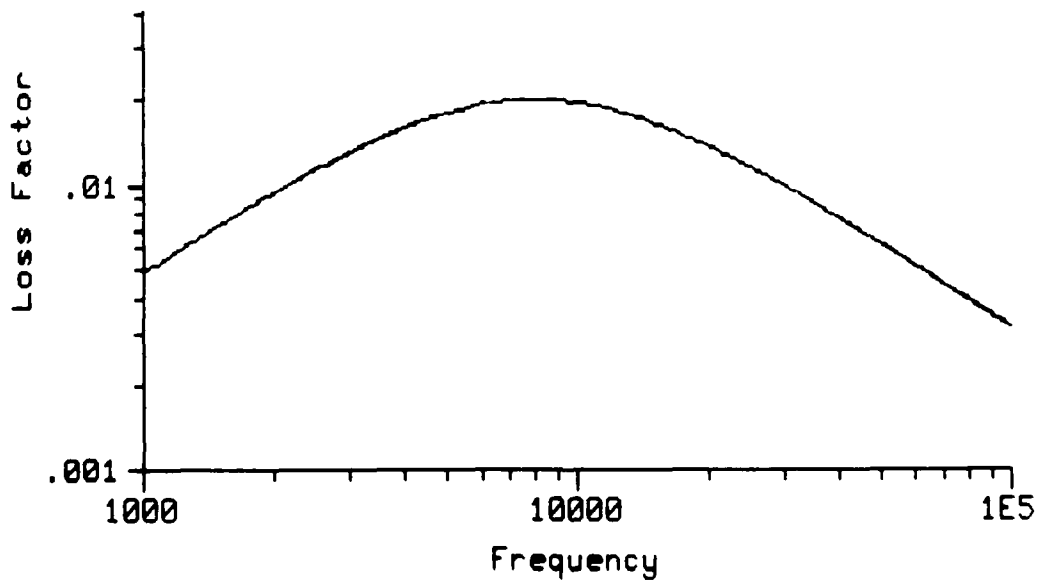

Figure 3. Loss Factor vs. Frequency for Single ATF Model

$E = 7.13 \times 10^{10}$ N/m^2
$B = 8000$ 1/s
$\alpha = 8000$ N/m^2
$\delta = 4.7766 \times 10^{6}$ M/m^2

As can be seen, damping peaks at a frequency of $\omega = B$ and tends toward zero at both high and low frequencies.

The power of the ATF model in the description of material damping can be seen as it is compared to other material damping models. It will be seen that the ATF model with no fractional derivatives can describe damping as modeled by the thermoelastic and classic viscoelastic damping models.

Comparison to the Thermoelastic Model. The linearized equations of dynamic coupled thermoelasticity are given in three dimensions as (Boley and Weiner, 1960:38)

$$\sigma_{ij} = \lambda \delta_{ij} \epsilon_{kk} + 2\mu \epsilon_{ij} - \alpha_T (3\lambda + 2\mu) \delta_{ij} (T - T_o) \quad (42)$$

$$\kappa T_{,ii} = c_v \dot{T} + (3\lambda + 2\mu) \alpha_T T_o \dot{\epsilon}_{kk} \quad (43)$$

with equilibrium requiring

$$\sigma_{ij,j} = \rho \ddot{u}_i \quad (44)$$

and compatibility conditions giving

$$\epsilon_{ij} = 1/2(u_{i,j} + u_{j,i}) \quad (45)$$

where

σ_{ij} = stress
ϵ_{ij} = strain
δ_{ij} = Kronecker delta
ρ = mass density
T = change in temperature from the initial, stress-free state
T_o = initial temperature, a constant
u_i = displacement
κ = thermal coductivity

c_v = specific heat at constant volume (per unit volume)

λ, μ = isothermal Lame's constants

α_T = coefficient of thermal expansion

Given a one-dimensional displacement with no shear the following conditions result:

$$u_1 = u_1(x,t)$$

$$u_2 = u_3 = 0$$

$$\sigma_{22} = \sigma_{33} = 0 \tag{46}$$

Compatibility, equation (45), results in

$$\epsilon_{11} = \partial u_1/\partial x \qquad \epsilon_{22} = \epsilon_{33} = 0 \tag{47}$$

and equilibrium gives

$$\rho \ddot{u} = \partial \sigma_{11}/\partial x = \partial \sigma_x/\partial x \tag{48}$$

Following application of the conditions of equation (46) to equation (42) we have

$$\sigma_{11} = (\lambda + 2\mu)\epsilon_{11} - \alpha_T(3\lambda + 2\mu)(T - T_o) \tag{49}$$

Equilibrium, equation (44), requires the derivative of equation (49) with respect to x. This, together with the result of applying equation (46) to equation (43), results in the linearized equations of dynamic coupled thermoelasticy for plane strain, as given by Boley and Weiner (Boley and Weiner, 1960:45-73):

$$\kappa T'' - c_v\dot{T} - (3\lambda + 2\mu)\alpha_T T_o \dot{u}' = 0$$

$$(\lambda + 2\mu)u'' - \rho\ddot{u} - (3\lambda + 2\mu)\alpha_T T' = 0 \tag{50}$$

Note that boundary condition effects are not included in this analysis.

For the case of the uniaxial rod considered in this thesis a set of conditions different than those of equations

(46) and (47) result:

$$\sigma_{22} = \sigma_{33} = 0$$

$$u_1 \neq 0,\ u_2 = 0,\ u_3 = 0$$

$$\epsilon_{11} = \partial u_1/\partial x$$

$$\epsilon_{22} = \epsilon_{33} = -\nu\epsilon_{11} \qquad (51)$$

where ν is Poisson's ratio. Equation (42) then gives

$$\sigma_{11} = \lambda(\epsilon_{11}+\epsilon_{22}+\epsilon_{33}) + 2\mu\epsilon_{11} - \alpha_T(T-T_o)(3\lambda+2\mu) \qquad (52)$$

Applying the last of the conditions of equation (51) results in the equation of stress in the x-direction:

$$\sigma_{11} = \lambda\epsilon_{11}(1 - 2\nu) + 2\mu\epsilon_{11} - \alpha_T(T - T_o)(3\lambda + 2\mu) \qquad (53)$$

Likewise, equation (43) results in

$$\kappa T'' = c_v\dot{T} + (3\lambda + 2\mu)\alpha_T T_o(1 - 2\nu)\dot{u}' \qquad (54)$$

Again, equilibrium is required, which results in the following from equation (53):

$$(\lambda + 2\mu - 2\nu)u'' - \alpha_T(3\lambda + 2\mu)T' - \rho\ddot{u} = 0 \qquad (55)$$

Recalling the definition of the isothermal Lame's constants, which involve the isothermal modulus, E_T,

$$\lambda = (\nu E_T)/[(1 + \nu)(1 - 2\nu)$$

$$\mu = E_T/[2(1 + \nu)] \qquad (56)$$

and substitution of equation (56) into equations (53) and (55) results in the equations of dynamic coupled thermoelasticity for the plane stress case of the uniaxial rod:

$$\kappa T'' - c_v\dot{T} - E_T\alpha_T T_o\dot{u}' = 0$$

$$E_T u'' - \rho\ddot{u} - E_T\alpha_T T' = 0 \qquad (57)$$

Taking the Fourier transform of equation (57), with spatial derivatives introducing ik and temporal derivatives introducing $i\omega$, results in the following equations:

$$\kappa(ik)^2\bar{T} - c_v(i\omega)\bar{T} - E_T\alpha_T T_o(ik)(i\omega)U = 0 \qquad (58)$$

$$E_T(ik)^2U - \rho(i\omega)^2U - E_T\alpha_T(ik)\bar{T} = 0 \qquad (59)$$

where U is the Fourier transform of u(x,t) and $\bar{T}$ is the Fourier transform of T(x,t). Solving equation (59) for $\bar{T}$, and substituting the result into equation (58) gives, after some algebraic manipulation,

$$\frac{\rho\omega^2}{k^2} = E_T\left[1 + \frac{(i\omega T_o E_T \alpha_T{}^2)/(\kappa k^2)}{1 + (i\omega c_v)/(\kappa k^2)}\right] \qquad (60)$$

This is in the form of the familiar complex modulus, with the right hand side of equation (60) being that modulus,

$$E^*(\omega) = E_T\left\{\frac{1 + i[\omega(c_v + \alpha_T{}^2 T_o E_T)/(\kappa k^2)]}{1 + i\omega[c_v/(\kappa k^2)]}\right\} \qquad (61)$$

which in turn can be compared to the complex modulus of the ATF model, equation (35), rewritten here for convenience:

$$E^*(\omega) = E\left[\frac{(1 - \Delta) + i(\omega/B)}{1 + i(\omega/B)}\right] \qquad (62)$$

Setting the right hand side of equation (61) equal to equation (62) results in the comparison equations which reveal values which the ATF model parameters must assume in order to model thermoelastic damping.

Comparison of the denominators of the two moduli results in the following equation:

$$B = (\kappa k^2)/c_v \qquad (63)$$

The real parts of the moduli's numerators results in the relationship

$$E(1 - \Delta) = E_T \tag{64}$$

This equation shows that the modulus, E, of the ATF model, when used to describe thermoelasticity, is related by an expression in Δ to the isothermal modulus, E_T.

Comparison of the imaginary parts of the numerators of the complex moduli resulting from the thermoelastic and ATF models gives the following relation:

$$E/B = (E_T c_v + \alpha_T^2 T_o E_T^2)/(\kappa k^2) \tag{65}$$

Substituting the expression for E found from equation (64), and the expression for B from equation (63) results in

$$(E_T c_v)/[(1 - \Delta)\kappa k^2] = (E_T c_v + \alpha_T^2 T_o E_T^2)/(\kappa k^2) \tag{66}$$

Solving this for Δ results in the value of Δ in terms of the thermoelastic parameters:

$$\Delta = (E_T \alpha_T^2 T_o)/(E_T \alpha_T^2 T_o + c_v) \tag{67}$$

Solving equation (64) for E with the value of Δ from equation (67) gives

$$E = E_T/(1 - \Delta) = [(E_T \alpha_T)^2 T_o + E_T c_v]/c_v \tag{68}$$

The ATF model, then, reproduces the thermoelastic model, given that the parameters of the ATF model are as follows:

$$1/B = c_v/(\kappa k^2)$$

$$\Delta = (E_T \alpha_T^2 T_o)/(E_T \alpha_T^2 T_o + c_v)$$

$$E = E_T[1 + (E_T T_o \alpha_T^2)/c_v] \tag{69}$$

It can be shown (Torvik, 1990; Appendix B) that the E of equation (69) is precisely the Young's modulus for an adiabatic deformation. Thus, $E = E_A$, and from equation (64)

$$\Delta = 1 - E_T/E_A \tag{70}$$

Invoking the definition of Δ, $\Delta = \delta^2/(E\alpha)$, gives

$$\delta^2 = \alpha(E_A - E_T) \tag{71}$$

Therefore, the free energy defined by equation (22) is seen to require that the coupling parameter, δ, of equation (22) be $\delta = [\alpha(E_A - E_T)]^{1/2}$. Likewise, the parameters α and E of equation (22) are the coefficient of thermal expansion and adiabatic modulus, repectively.

Comparison to the Viscoelastic Model. Recall that the generalized linear constitutive equation for a viscoelastic material is given by equation (8), repeated here for clarity:

$$\sum_{m=0}^{M} b_m d^m\sigma/dt^m = \sum_{n=0}^{N} a_n d^n\epsilon/dt^n \tag{72}$$

This can be written in the simplest case of viscous damping as

$$\sigma(t) = a_o\epsilon(t) + a_1 d\epsilon/dt \tag{73}$$

in which b_o is set to unity without loss of generality. In this case, a_o is the elastic modulus E_o. Using this in equation (72) results in

$$\sum_{m=1}^{M} b_m d^m\sigma/dt^m + \sigma(t) = E_o\epsilon(t) + \sum_{n=1}^{N} a_n d^n\epsilon/dt^n \tag{74}$$

Taking the Fourier transform of equation (74), where temporal derivatives introduce $(i\omega)$, with $\bar{\sigma}(\omega)$ and $\bar{\epsilon}(\omega)$ being the Fourier transforms of $\sigma(t)$ and $\epsilon(t)$, respectively, and dividing both sides of the result by $\bar{\epsilon}(\omega)$ results in an equation for the complex modulus:

$$E^*(\omega) = \frac{\bar{\sigma}(\omega)}{\bar{\epsilon}(\omega)} = \frac{E_o + \sum_{n=1}^{N} a_n (i\omega)^n}{1 + \sum_{m=1}^{M} b_m (i\omega)^m} \tag{75}$$

The complex modulus for the Kelvin solid includes only one term from the summation of the numerator, and the complex modulus becomes

$$E^*(\omega) = E_o + i(a_1\omega) \tag{76}$$

This model of viscoelasticity increases linearly with frequency. In turn, the model of a Maxwell fluid includes only one term from the summation in the denominator of equation (75), with the complex modulus given by

$$E^*(\omega) = E_o/(1 + i(b_1\omega)) \tag{77}$$

which, after multiplication of the complex modulus of the denominator, gives

$$E^*(\omega) = E_o(1 - ib_1\omega)/(1 + b^2\omega^2) \tag{78}$$

Taking one term from the summations of each of the numerator and denominator of equation (75) results in

$$E^*(\omega) = \frac{E_o + i\omega a_1}{1 + i\omega b_1} \tag{79}$$

Comparison of equation (79) to equation (35), the equation of the complex modulus for the single-ATF model, results in the following equations:

$$1/B = b_1$$

$$E(1 - \Delta) = E_\infty$$

$$E/B = a_1 \qquad (80)$$

This comparison is easily made, and the ATF model reduces to the viscoelastic model with 3 parameters -- E_∞, a_1, and b_1, if the constants are equated as follows:

$$B = 1/b_1 \qquad (81)$$

$$E = a_1/b_1 \qquad (82)$$

$$\Delta = 1 - (E_\infty b_1)/a_1 \qquad (83)$$

Inspection of equation (79) shows that the low frequency modulus must correspond to the isothermal elastic (rubbery) modulus. E_∞ is identified as such. Conversely, as the frequency goes to infinity, the real part of the modulus becomes a_1/b_1. Thus, this ratio is the adiabatic (glassy) modulus. Accordingly, the E used in the definition of the free energy must be the adiabatic modulus and the parameter Δ is

$$\Delta = 1 - E_T/E_A \qquad (84)$$

Recall from equation (36) that $\Delta = \delta^2/(E\alpha)$, so the coupling parameter, δ, must be

$$\delta = [\alpha(E_A - E_T)]^{1/2} \qquad (85)$$

III. Fractional Derivatives in the Description of Material Damping

Capitalizing on the previously made observation that the use of fractional derivatives in material models enables the description of material damping over a much broader frequency range, this research effort proposes to improve upon the accuracy of Lesieuture's model over a broader frequency range through the use of fractional derivatives. Coupled material constitutive relations will be developed using the concept of augmenting thermodynamic fields, with non-integer differentials allowed in the resulting partial differential equations.

Viscoelasticity Using the 4-Parameter Model. Bagley and Torvik have found the use of stress-strain laws, constitutive relationships, or equations of state which employ fractional or generalized derivatives to be valid as a material damping model (Torvik and Bagley, 1987). Relationships using a generalized derivative have been shown to have a sound theoretical basis, and are effective descriptors of the dynamic behavior of real materials. A brief review of Torvik and Bagley's work will be presented here.

Fractional Calculus. Ross presents a basic history of the fractional calculus, in which derivatives and integrals of fractional order are defined, and states that it is

nearly as old as the calculus of integer orders (Ross, 1977). The extended Riemann-Liouville definition of the generalized derivative is given as (Oldham and Spannier, 1974)

$$D^q[x(t)] = \frac{d^q x(t)}{d\tau^q} = \frac{1}{\Gamma(1-q)} \frac{d}{dt} \int_0^\infty \frac{x(t-\tau)}{\tau^q} d\tau \qquad (86)$$

for $0 \leq q < 1$. Γ is the gamma function, defined by

$$\Gamma(1-q) = \int_0^\infty e^{-x} x^{-q} dx \qquad (87)$$

At first glance, this would appear to be a formidable equation, yet when one considers the Fourier (or Laplace) domain, the generalized derivative manifests itself as a fractional power of ω (or s) (Caputo, 1976). The Fourier transform is defined as

$$F^T[x(t)] = \int_{-\infty}^\infty x(t) e^{-i\omega t} dt \qquad (88)$$

If $x(t) = 0$ for $t < 0$, then the Fourier transform can be written as

$$F^T[x(t)] = \int_0^\infty x(t) e^{-i\omega t} dt \qquad (89)$$

Taking the Fourier transform of the generalized derivative of equation (86) gives

$$F^T[D^q[x(t)]] = (i\omega)^q F^T[x(t)] \qquad (90)$$

The restriction placed on q is that it be a nonnegative real number less than one. For engineering applications, it is assumed that an irrational number can always be

approximated by a rational number, allowing for the restriction of q to being a rational number. Thus only fractional derivatives of rational order will be considered.

Fractional Derivatives in Viscoelastic Theory. The generalized differential operator form of the stress-strain constituitve equation is given by Christensen (Christensen, 1982:14) as

$$\sum_{m=1}^{M} b_m \frac{d^m \sigma(t)}{dt^m} + \sigma(t) = E\epsilon(t) + \sum_{n=1}^{N} a_n \frac{d^n \epsilon(t)}{dt^n} \qquad (91)$$

The Fourier transform of equation (91) yields

$$\sum_{m=1}^{M} b_m (i\omega)^m \bar{\sigma}(\omega) + \bar{\sigma}(\omega) = E\bar{\epsilon}(\omega) + \sum_{n=1}^{N} a_n (i\omega)^n \bar{\epsilon}(\omega) \qquad (92)$$

Through manipulation of this equation, a complex modulus is formed:

$$E^*(\omega) = \frac{\bar{\sigma}(\omega)}{\bar{\epsilon}(\omega)} = \frac{E + \sum_{n=1}^{N} a_n (i\omega)^n}{1 + \sum_{m=1}^{M} b_m (i\omega)^m} \qquad (93)$$

Now, if fractional derivatives are allowed in the general form of the relationship for linear viscoelasticity, the result is (Bagley and Torvik, 1979)

$$\sum_{m=1}^{M} b_m D^q[\sigma(t)] + \sigma(t) = E_o\epsilon(t) + \sum_{n=1}^{N} E_n D^q[\epsilon(t)] \qquad (94)$$

where q is a number between zero and one.

This is the form appropriate for a one-dimensional description of axial deformation. Many materials can be accurately modeled by replacing each sum in equation (94) by

a single term involving a fractional derivative

$$\sigma(t) + bD^q[\sigma(t)] = E_o\epsilon(t) + E_1D^q[\epsilon(t)] \qquad (95)$$

where b, q, E_o, and E_1 are the real parameters of this four parameter model (Bagley and Torvik, 1986). The Fourier transform of this model yields a complex modulus of the form

$$E^*(\omega) = \frac{E_o + E_1(i\omega)^q}{1 + b(i\omega)^r} \qquad (96)$$

with E_o and E_1/b being the rubbery and glassy moduli, repectively.

Thermodynamic constraints require the following conditions of the parameters of equation (96):

$$\begin{array}{ll} E_o \geq 0 & E_1 > 0 \\ b > 0 & E_1/b \geq 0 \end{array} \qquad (97)$$

These constraints insure a themodynamically well-behaved fractional calculus model of viscoelastic behavior (Bagley and Torvik, 1986).

Damping Ratio. In order to solve for the damping ratio, equation (96) must be further simplified using equations for complex numbers found in Appendix A. Using these simplifications, equation (96) may be rewritten as

$$E^*(\omega) = \frac{E_o + E_1(\omega)^q[\cos(q\pi/2) + i\ \sin(q\pi/2)]}{1 + b(\omega)^q[\cos(q\pi/2) + i\ \sin(q\pi/2)]} \qquad (98)$$

Letting $x = q\pi/2$ and multiplying equation (98) by the complex conjugate of the denominator results in the following for the complex modulus:

$$E^*(w) = N/D \qquad (99)$$

where

$$N = E_o + (E_o b + E_1)\omega^q \cos(x) + E_1 b\omega^{2q} + i\,[(E_1 - E_o b)\omega^q \sin(x)] \qquad (100)$$

and

$$D = 1 + 2b\omega^q \cos(x) + b^2\omega^{2q} \qquad (101)$$

Recall from equation (4) that the loss factor, η, equals the imaginary part of the complex modulus divided by its real part:

$$\eta = \frac{(E_1 - E_o b)\omega^q \sin(x)}{E_o + (E_o b + E_1)\omega^q \cos(x) + E_1 b\omega^{2q}} \qquad (102)$$

with the damping ratio being one-half the loss factor.

A plot of the loss factor versus the frequency of equation (102) is included as figure 4. Note the strong frequency dependence of the damping ratio. Also,

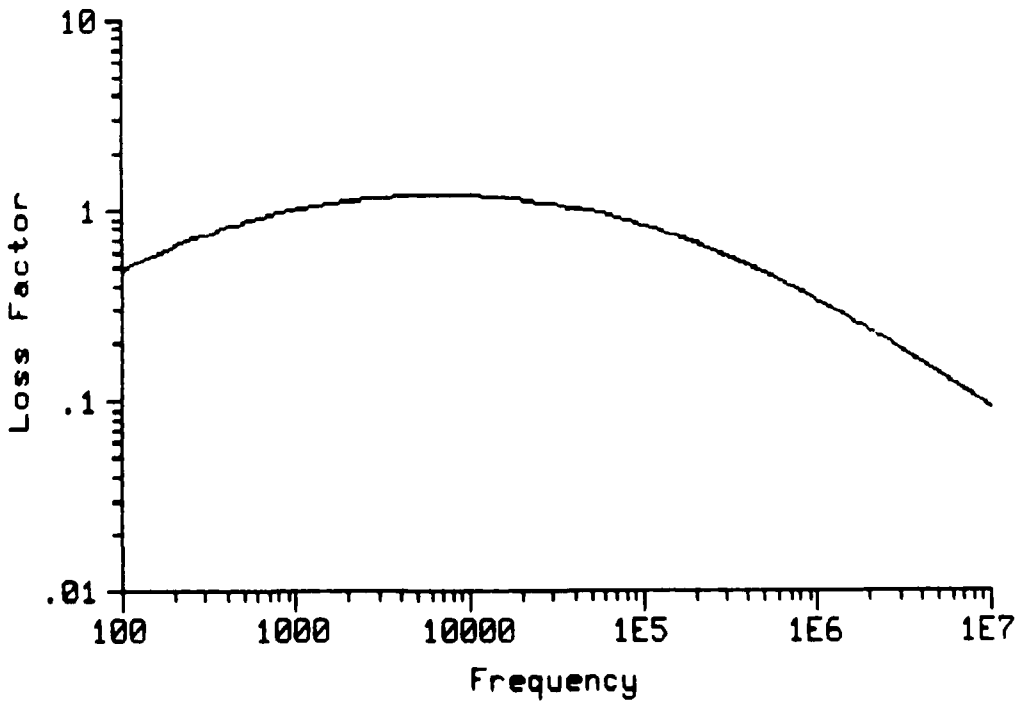

Figure 4. Loss Factor vs Frequency of 4-Parameter Fractional Derivative Model

examination of equation (97) shows that the thermodynamic constraints insure that the loss factor is positive for all frequencies (Bagley and Torvik, 1986). Values used for the plot of figure 4 are

$E_o = 5.04 \text{ X } 10^6 \text{ N/m}^2$
$E_1 = 2.27 \text{ X } 10^5 \text{ (N s)/m}^2$
$b = 2.80 \text{ X } 10^{-4} \text{ s}$
$q = 0.64$

These values correspond to Nitrile Rubber 1479 resulting from a "least-squares" fit to data previously obtained (Bagley and Torvik, 1986:137).

Single-ATF Model With Frational Derivatives. Torvik and Bagley (Torvik and Bagley, 1987:125) noted that most materials used in damping application are polymers showing a strong frequency dependence. The general viscoelastic relationships required to describe and adequately model this dependence usually require a large number of terms. They have noted that the frequency dependence of real materials is more closely approximated by models with fewer terms, but whose material constitutive time derivatives are of a fractional order. With four and five parameter models, they have accurately modeled material damping behavior over broad ranges of frequency, some even approaching eight decades.

Although Lesieutre declares this approach as "cumbersome," that is not the case and the ease of its use in application to the ATF model will be shown here.

Constitutive Equations. The equation for the Helmholtz free energy is as was used before, and can be found as equation (22). The fractional derivative will be applied to the equilibrium equation of irreversible thermodynamics as follows from equation (26):

$$\partial^q \xi/\partial t^q = -B(\xi - \bar{\xi}) = -B\xi + B\delta\epsilon/\alpha \qquad (103)$$

Here, we assume the rate process governing the restoration of the equilibrium state is a process of fractional order in time. This equation together with the balance of momentum relationship, equation (30), gives two coupled partial differential equations:

$$\rho\ddot{u} - Eu'' + \delta\xi' = 0$$

$$\partial^q \xi/\partial t^q + B\xi - B\delta u'/\alpha = 0 \qquad (104)$$

In the Fourier domain these equations become functions of ω. Taking the Fourier transform of equation (104) with time derivatives introducing $i\omega$ and spatial derivatives introducing ik gives

$$\rho(i\omega)^2 U - E(ik)^2 U + \delta(ik) Z = 0 \qquad (105)$$

$$(i\omega)^q Z + B Z - B\delta(ik)/\alpha U = 0 \qquad (106)$$

Solving equation (106) for Z results in

$$Z = iBk\delta/[\alpha B + \alpha(i\omega)^q] U \qquad (107)$$

Substituting equation (107) into equation (105) and canceling the U gives an equation that can be algebraically manipulated to give the complex modulus:

$$-\rho\omega^2 + Ek^2 - Bk^2\delta^2/[\alpha B + \alpha(i\omega)^q] = 0 \qquad (108)$$

Recall (Appendix A) that $(i\omega)^q$ can be written as

$$(i\omega)^q = \omega^q \left[\cos(q\pi/2) + i \sin(q\pi/2)\right] \tag{109}$$

Substituting $x = q\pi/2$ into equation (109) and the result into equation (108) results in

$$-\rho\omega^2 + Ek^2 - Bk^2\delta^2/\{\alpha[B+\omega^q\cos(x)-i\omega^q\sin(x)]\} = 0 \tag{110}$$

Algebraic manipulation of equation (110) results in a familiar form:

$$\frac{\rho\omega^2}{k^2} = E\left\{1 - \frac{\Delta}{1 + (\omega^q/B)[\cos(x) + i \sin(x)]}\right\} \tag{111}$$

where

$$\Delta = \delta^2/(E\alpha) \tag{112}$$

The right hand side of equation (111) is recognized as the complex modulus, which can be rewritten as

$$E^*(\omega) = E\left\{\frac{1 - \Delta + (\omega^q/B)[\cos(x) + i \sin(x)]}{1 + (\omega^q/B)[\cos(x) + i \sin(x)]}\right\} \tag{113}$$

Multiplying the numerator and denominator of the complex modulus of equation (113) by the complex conjugate of its denominator, $1 + (\omega^q/B)\cos(x) - i(\omega^q/B)\sin(x)$, results in the following after some algebraic manipulation:

$$E^*(\omega) = E\left\{1 - \Delta\left[\frac{1 + (\omega^q/B)\cos(x) - i\,(\omega^q/B)\sin(x)}{1 + 2(\omega^q/B)\cos(x) + \omega^{2q}/B^2}\right]\right\} \tag{114}$$

Damping Ratio. The loss factor can be found again from equation (4):

$$\eta = \frac{\Delta\,(\omega^q/B)\sin(x)}{1+2(\omega^q/B)\cos(x)+(\omega^q/B)^2-\Delta[1+(\omega^q/B)\cos(x)]} \tag{115}$$

Two assumptions are again made to arrive at the damping ratio. They are: (1) small damping, which in turns implies

that the damping ratio is half the loss factor, and (2) $\Delta << 1$, which will cancel all terms involving Δ from the denominator. This results in an equation for the damping ratio in terms of the frequency:

$$\zeta = \frac{(\delta^2/2E\alpha)\ (\omega^q/B)\ \sin(q\pi/2)}{1 + 2(\omega^q/B)\ \cos(q\pi/2) + (\omega^q/B)^2} \qquad (116)$$

By setting q of equation (115) equal to 1 the damping ratio reduces to that of Lesieutre's single-ATF model, since $\cos(q\pi/2)$ goes to zero and $\sin(q\pi/2)$ goes to one. The fractional derivative single-ATF model can then be considered a more general case of Lesieutre's model.

Figure 5 is a plot of the damping ratio versus frequency for three values of q in the fractional derivative

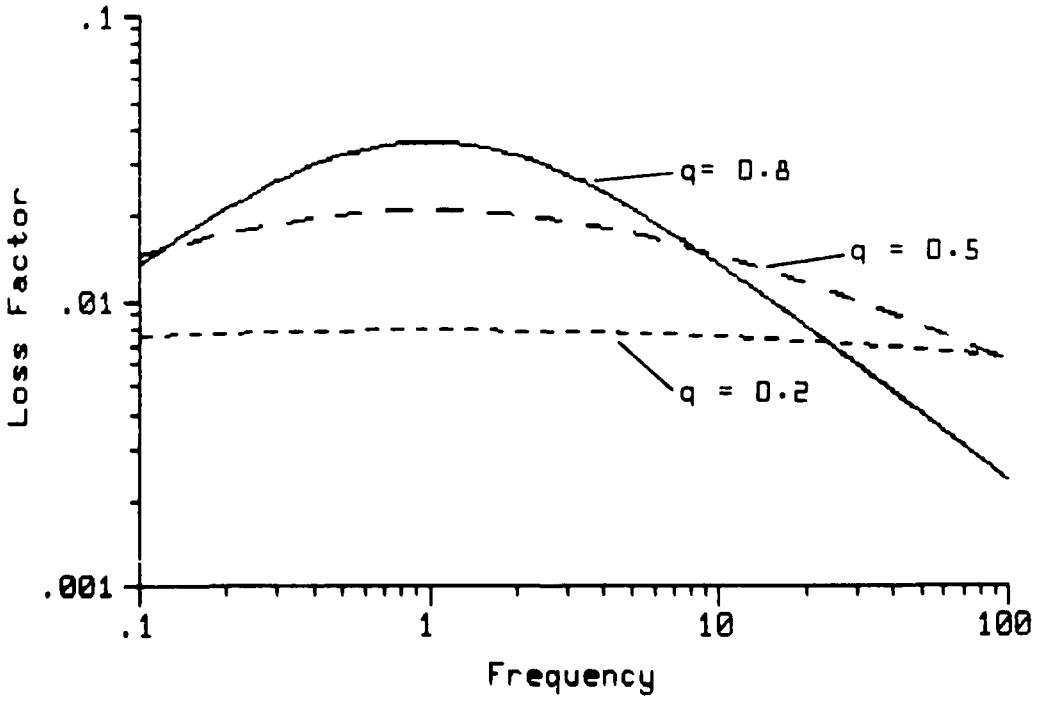

Figure 5. Single ATF Model with Fractional Derivatives

single-ATF model. Values for the other parameters were as follows:

$B = 1.0$
$\Delta = 0.1$

As the value of q decreases the curve flattens out, as well as opening up.

Complex Modulus Formulation. An alternate method of arriving at the loss factor, and thus, the damping ratio, might be termed the "complex modulus" formulation. Starting with equations (24) and (103) results in, after the Fourier transform:

$$\bar{\sigma}(\omega) = E\bar{\epsilon}(\omega) - \delta Z(\omega) \tag{117}$$

$$(i\omega)^q Z(\omega) = -BZ(\omega) + (B\delta/\alpha)\epsilon(\omega) \tag{118}$$

where $\bar{\sigma}(\omega)$ is the Fourier transform of $\sigma(x,t)$, $\bar{\epsilon}(\omega)$ is the Fourier transform of $\epsilon(x,t)$, and $Z(\omega)$ is the Fourier transform of $\xi(x,t)$. Solve equation (118) for $Z(\omega)$:

$$Z(\omega) = \{B\,\delta / [\alpha B + \alpha(i\omega)^q]\}\,\epsilon(\omega) \tag{119}$$

Substituting the result into equation (117) and dividing by $\bar{\epsilon}(\omega)$ results in an equation for the complex modulus:

$$\bar{\sigma}(\omega)/\bar{\epsilon}(\omega) = E - B\delta^2/[\alpha B + \alpha(i\omega)^q] \tag{120}$$

Recalling $i^q = \cos(q\pi/2) + i\sin(q\pi/2)$ and letting $x = q\pi/2$, equation (120) becomes

$$\frac{\bar{\sigma}(\omega)}{\bar{\epsilon}(\omega)} = E\left\{1 - \Delta\left[\frac{1}{1+(\omega^q/B)\cos(x)+i(\omega^q/B)\sin(x)}\right]\right\} \tag{121}$$

where Δ is defined as before in equation (112). This is the complex modulus. After multiplying the numerator and

denominator of the innermost term by the denominator's complex conjugate, equation (121) takes on the familiar form of equation (114):

$$E^*(\omega) = E\left\{1 - \Delta\left[\frac{1+(\omega^q/B)\cos(x)-i(\omega^q/B)\sin(x)}{1 + 2(\omega^q/B)\cos(x) + (\omega^q/B)^2}\right]\right\} \qquad (122)$$

Derivation of the damping ratio from this point follows the previous derivation.

Comparison of the ATF model with Fractional Derivatives to the 4-Parameter Model. Recall from equation (98) that the expression for the complex modulus of the four parameter model of viscoelasticity is

$$E^*(\omega) = \frac{E_0 + E_1\omega^r[\cos(y) + i\,\sin(y)]}{1 + b\omega^r[\cos(y) + i\,\sin(y)]} \qquad (123)$$

where $y = r\pi/2$ from the derivation of equation (98).

Equation (123) can now be compared to equation (113), the equation of the complex modulus for the single-ATF model with fractional derivatives. The following equations of comparison result:

$$1 + (\omega^q/B)[\cos(x) + i\,\sin(x)] = 1 + (b\omega^r)[\cos(y) + i\,\sin(y)] \qquad (124)$$

$$E(1 - \Delta) = E_0 \qquad (125)$$

$$E(\omega^q/B)[\cos(x) + i\,\sin(x)] = (E_1\omega^r)[\cos(y) + i\,\sin(y)] \qquad (126)$$

Examination of all equations show that r must equal q in order for the terms involving ω and the trigonometric

functions to equate. Therefore, the first equivalency equation is

$$r = q \tag{127}$$

which in turn implies $x = y$.

Substituting equation (127) into equation (124) and solving for B shows that the second condition for model equivalency is

$$B = 1/b \tag{128}$$

Using equation (128) in equation (126) gives the relationship:

$$E/B = E_1 \tag{129}$$

The final relationship of comparison is that of equation (125), repeated here for clarity:

$$E(1 - \Delta) = E_o \tag{130}$$

Equations (127) through (130) are the equations that show equivalency between the 4-Parameter model and the ATF model with fractional derivatives. It should be noted that no assumptions were made as to small Δ. Recall that the glassy modulus equals

$$E_g = E_1/b = (E/B)/(1/B) = E \tag{131}$$

Comparing this to the equation for the rubbery modulus, equation (131) shows that the ratio of the glassy modulus to the rubbery modulus is

$$E_g/E_o = E/[E(1 - \Delta)] \tag{132}$$

In many materials the glassy modulus is three orders of

magnitude larger than the rubbery modulus. This being the case, Δ must equal 0.999 or greater.

As can be seen, Δ is not small as compared to one in this case. Bagley and Torvik have used the 4-Parameter model to produce curves with accurate results over a very broad frequency range for many materials, principally polymers. The assumptions that $\Delta << 1$, then, is inapproriate for use with 4-parameter viscoelastic modeling.

For comparison purposes, the plot of the loss factor versus frequency for the single-ATF model without the small Δ assumption is shown as figure 6. The values used for the plot are as follows:

B = 1
Δ = 0.9995

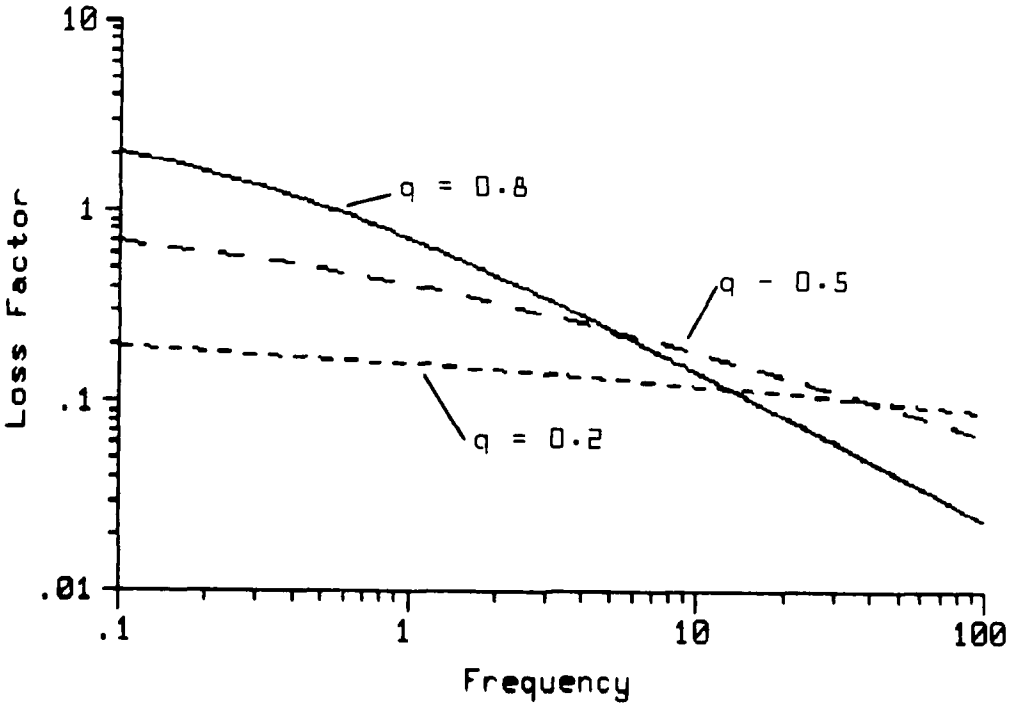

Figure 6. Single-ATF Model Without Small Δ Assumption

No cancellation of Δ from the denominator of the loss factor was made in producing figure 6. Figure 7, for comparison purposes, is a plot of the loss factor using the same values of B and Δ, but with denominator terms involving Δ canceled.

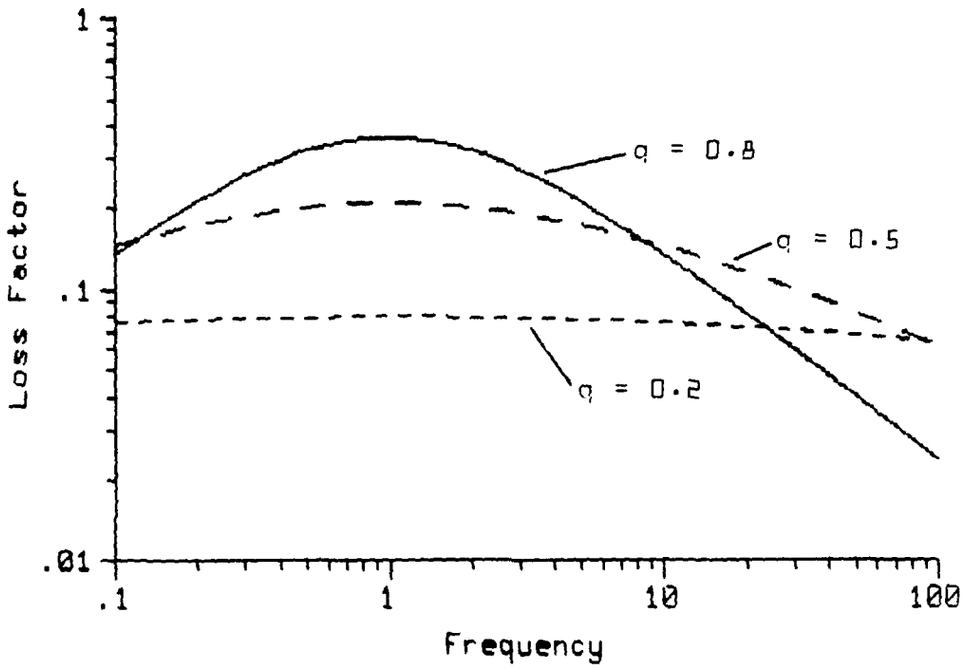

Figure 7. Single-ATF Model With Small Δ Assumption

IV. Two-ATF Model

Lesieutre's development of the model for the one-dimensional vibration of an isotropic rod was selected for ease of illustration of the ATF modeling method. He states that in practice additional augmenting thermodynamic fields can be used as needed to better approximate experimental data over the frequency range of interest (Lesieutre, 1989:19). In order to illustrate the ease or difficulty of adding additonal ATFs, the following developments of two-ATF models were performed.

Two-ATF Model with Integer-order Derivatives. For the development of the two-ATF model with integer-order derivatives a second augmenting thermodynamic field is added to the free energy equation. The formulation of the damping ratio followed that of Lesieutre's single-ATF model, with the addition of equations involving the second ATF.

Constitutive Equations. Once again, the Helmholtz free energy is employed to arrive at the constituitive equations. We hypothesize

$$f = 1/2E\epsilon^2 + 1/2\alpha_1\xi_1^2 + 1/2\alpha_2\xi_2^2 - \delta_1\epsilon\xi_1 - \delta_2\epsilon\xi_2 - \alpha_3\xi_1\xi_2 \qquad (133)$$

Here, ϵ is the strain field, ξ_1 and ξ_2 are the two augmenting thermodynamic fields, δ_1 and δ_2 are the strengths of the coupling between strain and ξ_1 and ξ_2, respectively, and α_3 is the strength of the coupling between the two ATFs, ξ_1 and ξ_2.

The stress field is again found from the relation

$$\sigma = \partial f/\partial \epsilon = E\epsilon - \delta_1 \xi_1 - \delta_2 \xi_2 \qquad (134)$$

and the two affinities A_1 and A_2 can be found using equation (25), which results in

$$A_1 = -\partial f/\partial \xi_1 = \delta_1 \epsilon - \alpha_1 \xi_1 + \alpha_3 \xi_2 \qquad (135)$$

$$A_2 = -\partial f/\partial \xi_2 = \delta_2 \epsilon - \alpha_2 \xi_2 + \alpha_3 \xi_1 \qquad (136)$$

Assuming the irreversible thermodynamic processes are described by first order rate equations, the time rate of change of ξ_i, or $\partial \xi_i/\partial t$ is assumed to be proportional to the deviation from an equilibrium value:

$$\partial \xi_i/\partial t = -B_i(\xi_i - \bar{\xi}_i) \qquad i=1,2 \qquad (137)$$

with the value of $\bar{\xi}_i$ found from the value of ξ_i at equilibrium, or when the affinity is zero. Here it is assumed that there is no coupling between the two ATFs in the equilibrium relationship of equation (137), which would be indicated by an equation of the form

$$\partial \xi_1/\partial t = -B_1(\xi_1 - \bar{\xi}_1) - C_1(\xi_2 - \bar{\xi}_2) \qquad (138)$$

for the first ATF, with a similar equation for the second ATF. Such interaction are not used in the developments of the two-ATF models.

Setting A_1 in equation (135) equal to zero and solving for ξ_1 gives

$$\bar{\xi}_1 = \delta_1 \epsilon/\alpha_1 + \alpha_3 \xi_2/\alpha_1 \qquad (139)$$

Similarly, for $\bar{\xi}_2$,

$$\bar{\xi}_2 = \delta_2 \epsilon/\alpha_2 + \alpha_3 \xi_1/\alpha_2 \qquad (140)$$

Substituting these results into equation (137) gives, for

the time dependence of the ATFs, two equations:

$$\partial\xi_1/\partial t = -B_1(\xi_1 - \delta_1\epsilon/\alpha_1 - \alpha_3\xi_2/\alpha_1) \quad (141)$$

$$\partial\xi_2/\partial t = -B_2(\xi_2 - \delta_2\epsilon/\alpha_2 - \alpha_3\xi_1/\alpha_2) \quad (142)$$

Notice that now ξ_1 and ξ_2 are coupled in ξ_1 and ξ_2, as well as in strain, ϵ.

Balance of linear momentum requires that, for a one-dimensional deformation,

$$\partial\sigma/\partial x - \rho\partial^2 u/\partial t^2 = 0 \quad (143)$$

The derivative of equation (134) with respect to x gives

$$\partial\sigma/\partial x = E\partial\epsilon/\partial x - \delta_1\partial\xi_1/\partial x - \delta_2\partial\xi_2/\partial x \quad (141)$$

which, when substituted into equation (143) and recalling $\epsilon(x,t) = \partial u(x,t)/\partial x = u'$, results in a partial differential equation coupled in u, ξ_1, and ξ_2:

$$\rho\ddot{u} - Eu'' + \delta_1\xi_1' + \delta_2\xi_2' = 0 \quad (145)$$

where the dots represent time derivatives and the primes represent spatial derivatives. This equation together with equations (141) and (142) are the governing equations for longitudinal oscillations of an axial rod.

<u>Damping Ratio</u>. In order to solve the constitutive equations with greater ease, the Fourier transform is invoked, with time derivatives introducing $i\omega$, and spatial derivatives introducing ik, which results in the following equations:

$$\begin{aligned} &\rho(i\omega)^2U - E(ik)^2U + \delta_1(ik)Z_1 + \delta_2(ik)Z_2 = 0 \\ &B_1\delta_1(ik)U - \alpha_1(B_1 + i\omega)Z_1 + B_1\alpha_3Z_2 = 0 \\ &B_2\delta_2(ik)U + B_2\alpha_3Z_1 - \alpha_2(B_2 + i\omega)Z_2 = 0 \end{aligned} \quad (146)$$

These equations may be expressed in matrix form as

$$\begin{bmatrix} -\rho\omega^2 + Ek^2 & i\delta_1 k & i\delta_2 k \\ iB_1\delta_1 k & -\alpha_1(B_1 + i\omega) & B_1\alpha_3 \\ iB_2\delta_2 k & B_2\alpha_3 & -\alpha_2(B_2 + i\omega) \end{bmatrix} \begin{Bmatrix} U \\ Z_1 \\ Z_2 \end{Bmatrix} = \{\underline{0}\} \quad (147)$$

This is a linear system of equations whose solution is determined by finding the determinant of the matrix and setting it equal to zero:

$$(-\rho\omega^2 + Ek^2)[(-\alpha_1)(B_1 + i\omega)(-\alpha_2)(B_2 + i\omega) - B_1B_2\alpha_3{}^2]$$
$$- ik\delta_1[iB_1k\delta_1(-\alpha_2)(B_2 + i\omega) - iB_1B_2k\alpha_3\delta_2]$$
$$+ ik\delta_2[iB_1k\delta_1(B_2\alpha_3) + iB_2k\alpha_1\delta_2(B_1 + i\omega)] = 0 \quad (148)$$

Carrying out the algebra and rearranging equation (148) gives

$$(-\rho\omega^2 + Ek^2)[\gamma - \omega^2/(B_1B_2) + i\omega/B_3]$$
$$- k^2E[\Delta_1 + \Delta_2 + \Delta_3 + i\omega(\Delta_1/B_2 + \Delta_2/B_1)] = 0 \quad (149)$$

where

$$\gamma = 1 - \alpha_3{}^2/(\alpha_1\alpha_2)$$
$$\Delta_1 = \delta_1{}^2/(E\alpha_1)$$
$$\Delta_2 = \delta_2{}^2/(E\alpha_2)$$
$$\Delta_3 = 2(\delta_1\delta_2\alpha_3)/(E\alpha_1\alpha_2)$$
$$1/B_3 = 1/B_1 + 1/B_2 \quad (150)$$

Dividing equation (149) by $\gamma - \omega^2/(B_1B_2) + i\omega/B_3$, dividing the result by ρ, and factoring k^2/ρ from this results in an equation from which the complex modulus can be derived:

$$-\omega^2 + \frac{k^2}{\rho}\left\{E - \frac{E[\Delta_1 + \Delta_2 + \Delta_3 + i\omega(\Delta_1/B_2 + \Delta_2/B_1)]}{\gamma - \omega^2/(B_1B_2) + i\omega/B_3}\right\} = 0 \quad (151)$$

The bracketed quantity of equation (151) is the complex modulus $E^*(\omega)$, and the loss factor η, therefore, can be found from equation (4). Multiplying the complex modulus by the complex conjugate, $\gamma - \omega^2/(B_1B_2) - i\omega/B_3$, of the denominator of the second term within the brackets of equation (151) results in the following expression for the complex modulus:

$$E^*(\omega) = E\left\{\frac{N_{re} + i\,N_{im}}{[\gamma - \omega^2/(B_1B_2)]^2 + (\omega/B_3)^2}\right\} \tag{152}$$

where

$$N_{re} = [\gamma - \omega^2/(B_1B_2)][\gamma - \omega^2/(B_1B_2) + \Delta_1 + \Delta_2 + \Delta_3] + (\omega/B_3)(\Delta_1\omega/B_2 + \Delta_2\omega/B_1 + \omega/B_3) \tag{153}$$

and

$$N_{im} = [\gamma - \omega^2/(B_1B_2)][\Delta_1\omega/B_2 + \Delta_2\omega/B_1] - (\omega/B_3)(\Delta_1 + \Delta_2 + \Delta_3) \tag{154}$$

The loss factor, found using equation (4), is given by

$$\eta = Im\{E^*(\omega)\}/Re\{E^*(\omega)\} = N_{im}/N_{re} \tag{155}$$

where N_{im} and N_{re} are given by equations (154) and (153), respectively.

With the assumptions that damping is small, and that $\Delta_1 << 1$, $\Delta_2 << 1$, and $\Delta_3 << 1$, the damping ratio then becomes

$$\zeta = \frac{(\omega/B_3)(\Delta_1+\Delta_2+\Delta_3) - [\gamma-\omega^2/(B_1B_2)][\omega\Delta_1/B_2+\omega\Delta_2/B_1]}{2\{[\gamma - \omega^2/(B_1B_2)]^2 + (\omega/B_3)^2\}} \tag{156}$$

In order to check that this reduces to the case when only one ATF was used, set $\alpha_3 = 0$ and $\delta_2 = 0$, which from equation (150) assures $\Delta_2 = \Delta_3 = 0$ and $\gamma = 1$. Equations (153) and (154) then become

$$N_{rel} = 1 - (2\omega^2)/(B_1B_2) + \omega^4/(B_1B_2)^2 + (\omega^2\Delta_1)/(B_2B_3) + \omega^2/B_3^2 \quad (157)$$

$$N_{iml} = \Delta_1\omega[1/B_2 - \omega/(B_1B_2^2) - 1/B_3] \quad (158)$$

and the loss factor is an equation in terms of Δ_1, B_1, and B_2, with no coupling between the second ATF, ξ_2, and the strain, ϵ, or the first ATF, ξ_1. The loss factor is then

$$\eta = N_{iml}/N_{rel} = \frac{\omega\Delta_1(B_1+B_2)/(B_1B_2) - [1 - \omega^2/(B_1B_2)][\omega\Delta_1/B_2]}{[1-\omega^2/(B_1B_2)]^2 + [\omega(B_1+B_2)/(B_1B_2)]^2} \quad (159)$$

As can be seen, equation (159) is not equivalent to twice equation (41), the loss factor for a single ATF, in that the material constant B_2 is still present. Taking the limit of equation (159) as B_2 goes to infinity results in

$$\eta = \frac{\omega\Delta_1/B_1}{1 + \omega^2/B_1^2} \quad (160)$$

Examination of equation (160) shows it to be identical to the value of the loss factor for the case where only one ATF was employed. The loss factor of the two ATF model, therefore, reduces to that of the one ATF model exactly.

Characteristics of the Two-ATF Model. Figure 8 is a plot of the loss factor versus frequency for the two ATF model with the values of the parameters as follows:

$B_1 = 1$
$B_2 = 10$
$\Delta_1 = 0.1$
$\Delta_2 = 0.05$

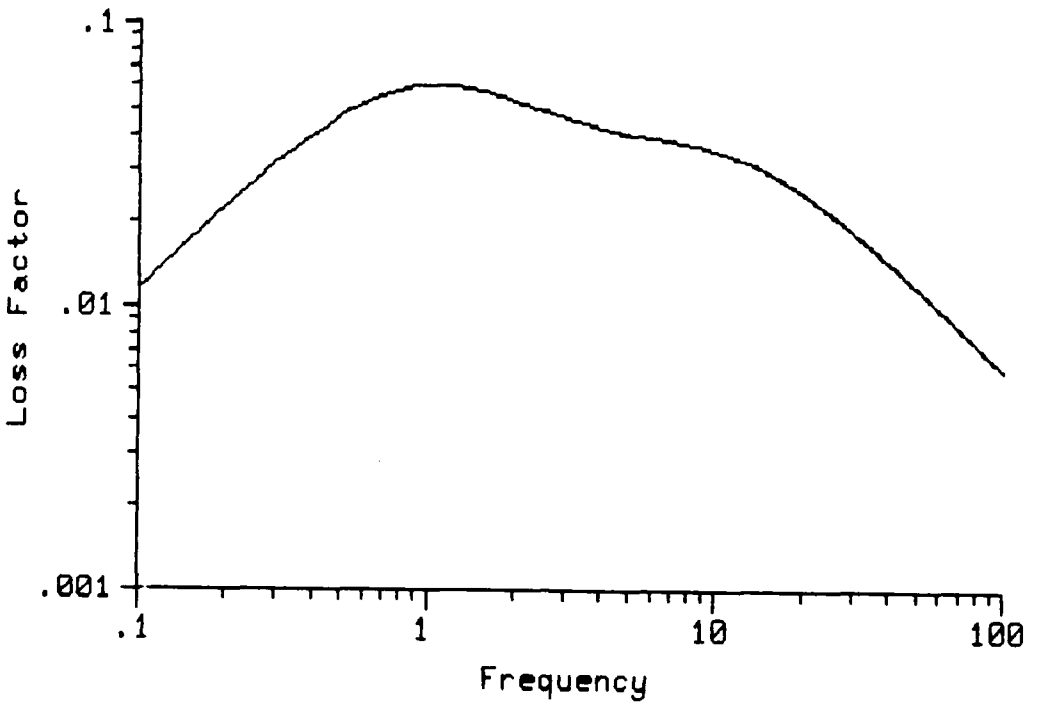

Figure 8. Loss Factor vs. Frequency - 2-ATF Model

Here B_1 and B_2 have the dimensions of frequency, and Δ_1 and Δ_2 are dimensionless. These values were selected only to allow for ease in comparison as the parameters of the model are changed. Again, α_1 and α_2 are assigned values equivalent to the magnitudes of B_1 and B_2, respectively (Lesieutre, 1989:48, 146).

It will be noted that Δ_3 is a function of δ_1 and δ_2, as well as α_1, α_2, and α_3. From equation (150)

$$\delta_1 = (\Delta_1 E \alpha_1)^{1/2} \tag{161}$$

$$\delta_2 = (\Delta_2 E \alpha_2)^{1/2} \tag{162}$$

$$\Delta_3 = \frac{\delta_1 \delta_2 \alpha_3}{E\alpha_1\alpha_2} = \frac{\alpha_3 (\Delta_1 \Delta_2 \alpha_1 \alpha_2)^{1/2}}{\alpha_1 \alpha_2}$$

$$= \left(\frac{\Delta_1 \Delta_2}{\alpha_1 \alpha_2} \right)^{1/2} \alpha_3 \qquad (163)$$

α_3, then, can be found from a relationship of α_1 and α_2:

$$\alpha_3 = C^* \ (\alpha_1 \alpha_2)^{1/2} \qquad (164)$$

and

$$\Delta_3 = C^* \ (\Delta_1 \Delta_2)^{1/2} \qquad (165)$$

where C^* is a constant parameter that can be varied as the other material parameters. For the plot in Figure 8 C^* was set equal to 0.1, and $\Delta_3 = \sqrt{5} \times 10^{-2}$.

Figure 8 shows the "double hump" characteristic of the loss factor when two ATFs are employed, with the peak of the first maximum at a frequency equal to the value of B_1 and the second maximum falling on a frequency equal to the value of B_2. Notice that two maxima are discernable, although they almost merge into a single curve. This discernability is not clearly the case in some of the later plots.

Figures 9 through 18 are plots of the loss factor versus frequency with different parameters of the two-ATF model varied for each plot.

Figure 6 shows the loss factor versus frequency with B_1=0.2. The first maximum has shifted to the left and corresponds to a frequency of 0.2. The two maxima can be seen as separate maxima. This is also obvious in figure 10, in which the value of B_2 is increased to 90. Again, the

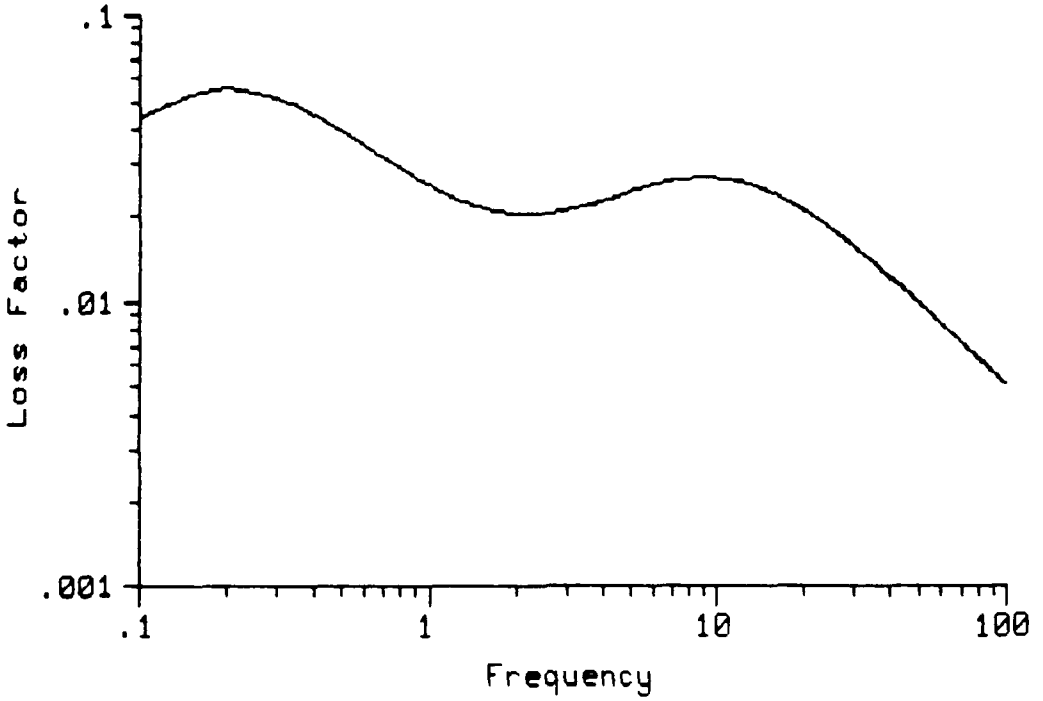

Figure 9. Two-ATF Model with $B_1=0.2$
($B_2=10$, $\Delta_1=0.1$, $\Delta_2=0.05$, $\Delta_3=\sqrt{5}$ X 10^{-2})

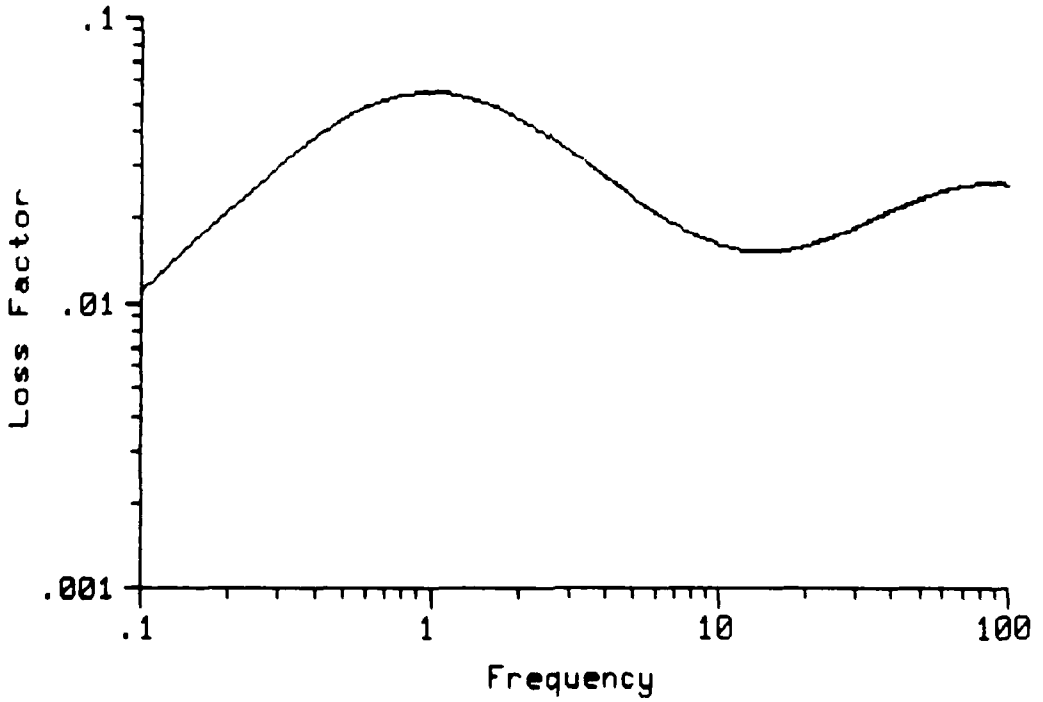

Figure 10. Two-ATF Model with $B_2=90$
($B_1=1$, $\Delta_1=0.1$, $\Delta_2=0.05$, $\Delta_3=\sqrt{5}$ X 10^{-2})

second maximum shifts to a value corresponding to 90. Decreasing the value of B_1 also tends to decrease the maximum value of the loss factors for both peaks of the curve, which also occurs with an increase in B_2.

The opposite effect is apparent as B_1 is increased to 9.0 and B_2 is decreased to 2 in figures 11 and 12, respectively. As the values of B_1 and B_2 approach each other, the double hump collapses into one maximum, and the value of the loss factor tends to increase. In both cases the value of the maximum is the same, with the curve appearing to be the same, only shifted along the x-axis.

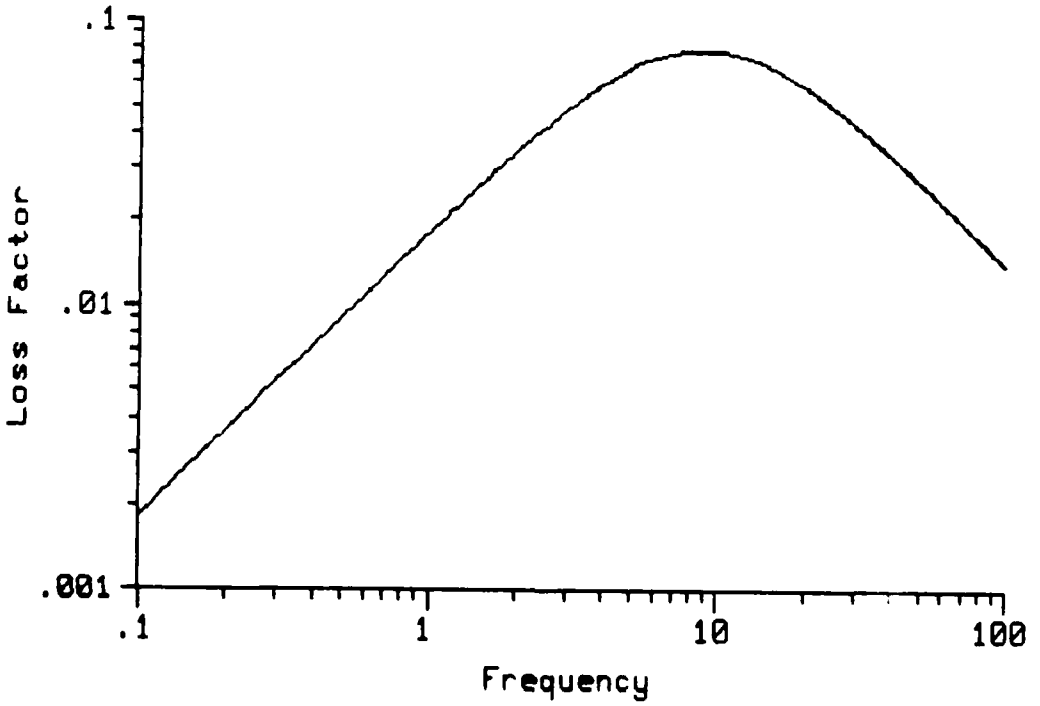

Figure 11. Two-ATF Model with B_1=9.0 (B_2=10, Δ_1=0.1, Δ_2=0.05, $\Delta_3=\sqrt{5} \times 10^{-2}$)

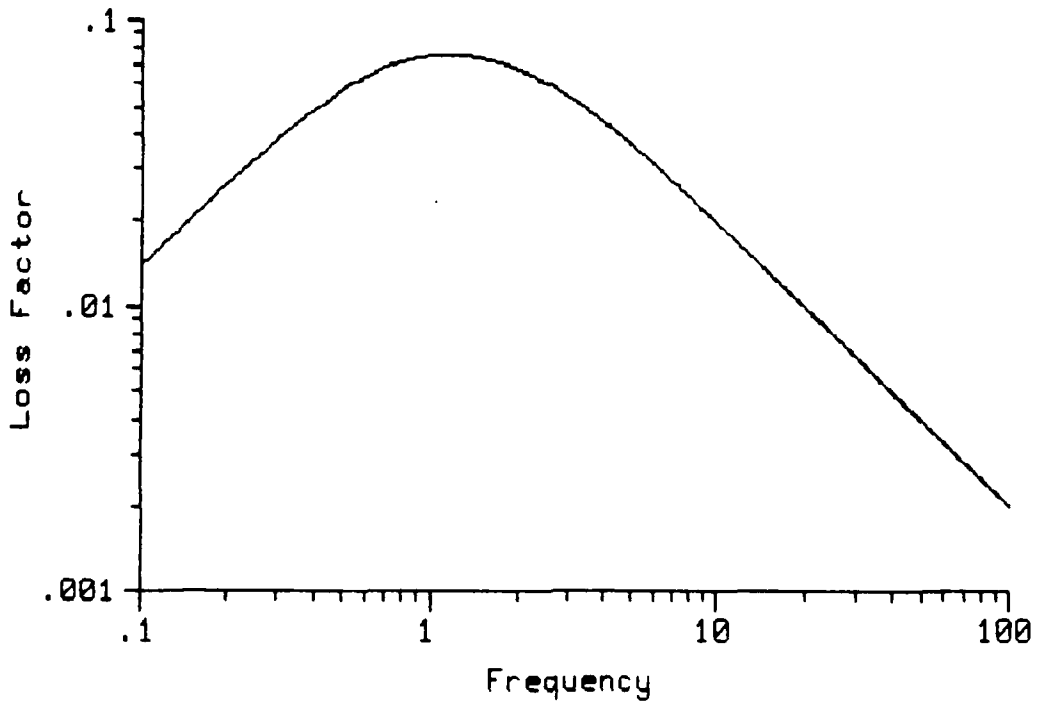

Figure 12. Two-ATF Model with B_2=2.0
(B_1=1, Δ_1=0.1, Δ_2=0.05, $\Delta_3=\sqrt{5} \times 10^{-2}$)

Figures 13 and 14 show the effects of varying Δ_1, with figure 13 corresponding to an increase of Δ_1 to 0.9, and figure 14 to a decrease to 0.02. An increase of Δ_1 tends to collapse the separate maxima into one peak and to increase the value of the loss factor at that maximum. The value of the maximum loss factor is almost an order of magnitude higher. Although barely perceptible, an inflection point, or local maximum, occurs at the frequency corresponding to B_2. With a decrease in Δ_1, however, a decrease in the maximum value corresponding to B_1 occurs. This decrease is not an order of magnitude as was the case with the increase. The value of the maximum at $\omega = B_2$ decreases as well, but remains the dominant peak.

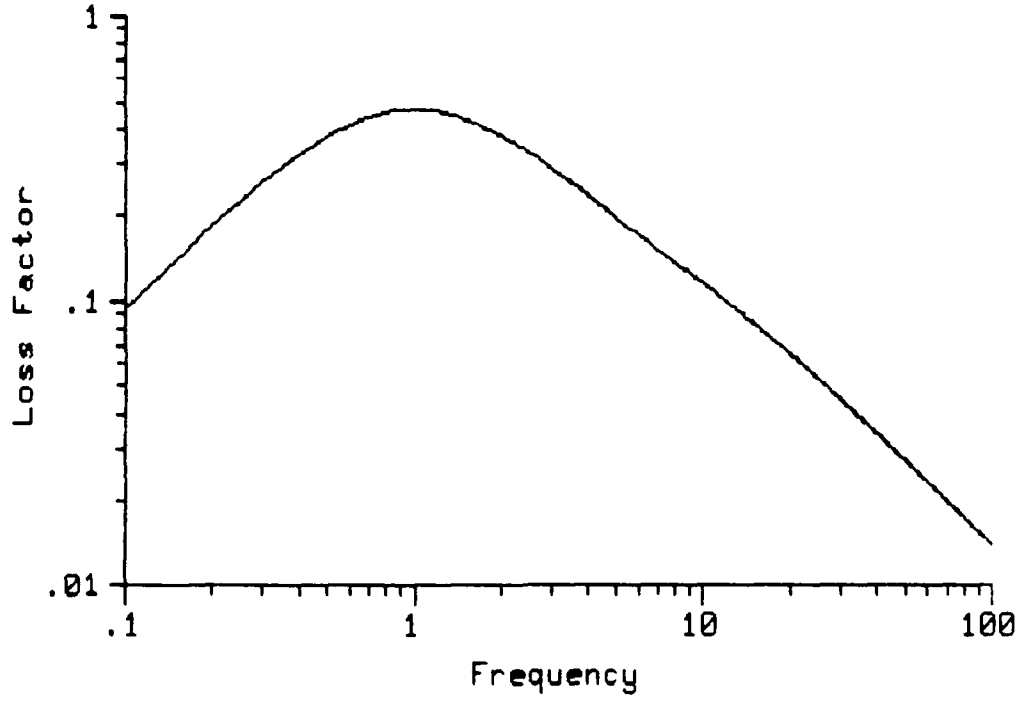

Figure 13. Two-ATF Model with Δ_1=0.9
(B_1=1, B_2=10, Δ_2=0.05, $\Delta_3=\sqrt{5}$ X 10^{-2})

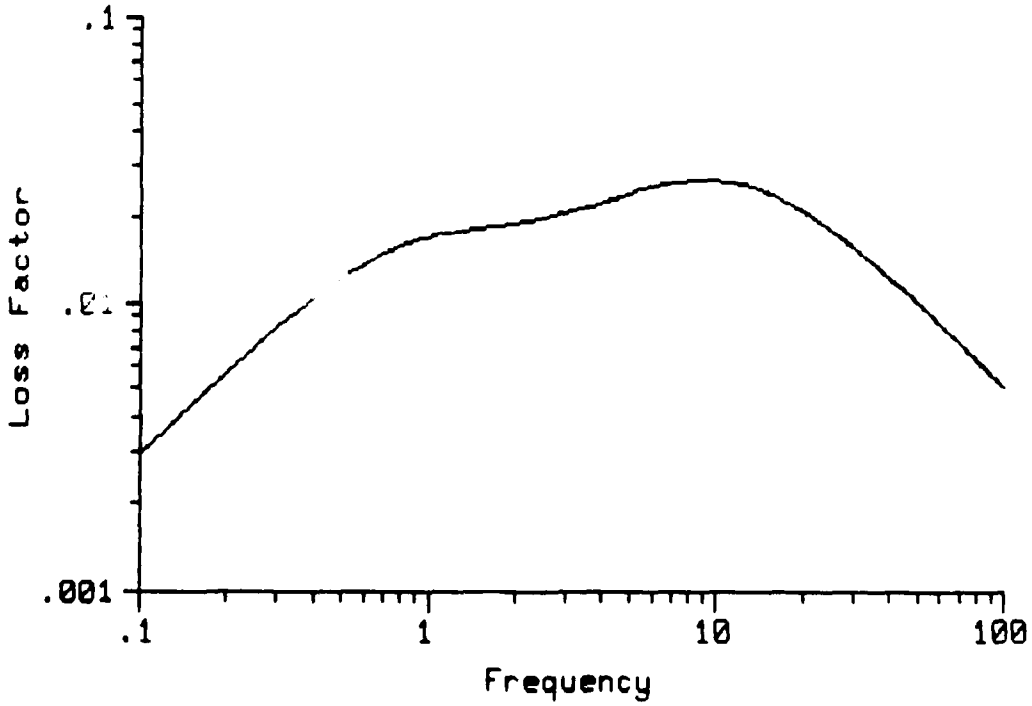

Figure 14. Two-ATF Model with Δ_1=0.02
(B_1=1, B_2=10, Δ_2=0.05, $\Delta_3=\sqrt{5}$ X 10^{-2})

Figures 15 and 16 show similar results as Δ_2 is decreased to 0.005, with the peaks merging into one dominant maximum, and as Δ_2 is increased to 0.5. In figure 15, the value of the loss factor at this maximum is only slightly less than that of figure 8, while the value of the loss

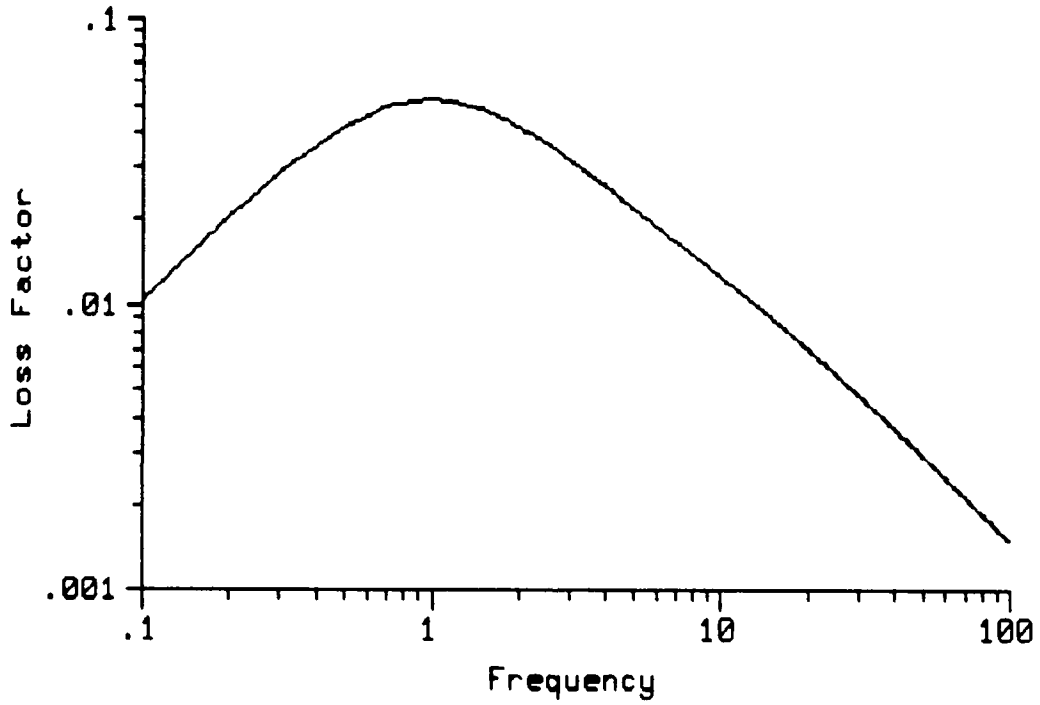

Figure 15. Two-ATF Model with Δ_2=0.005
(B_1=1, B_2=10, Δ_1=0.1, $\Delta_3=\sqrt{5}$ X 10^{-2})

factor at the second maximum, barely discernable at a frequency of 10 more as a deflection point, is considerably lower. Figure 16 shows the loss factor being greater over the entire frequency range, with the maximum at a frequency of 10 being dominant. As the difference between Δ_1 and Δ_2 increases, the double maxima merge to one maximum whose peak

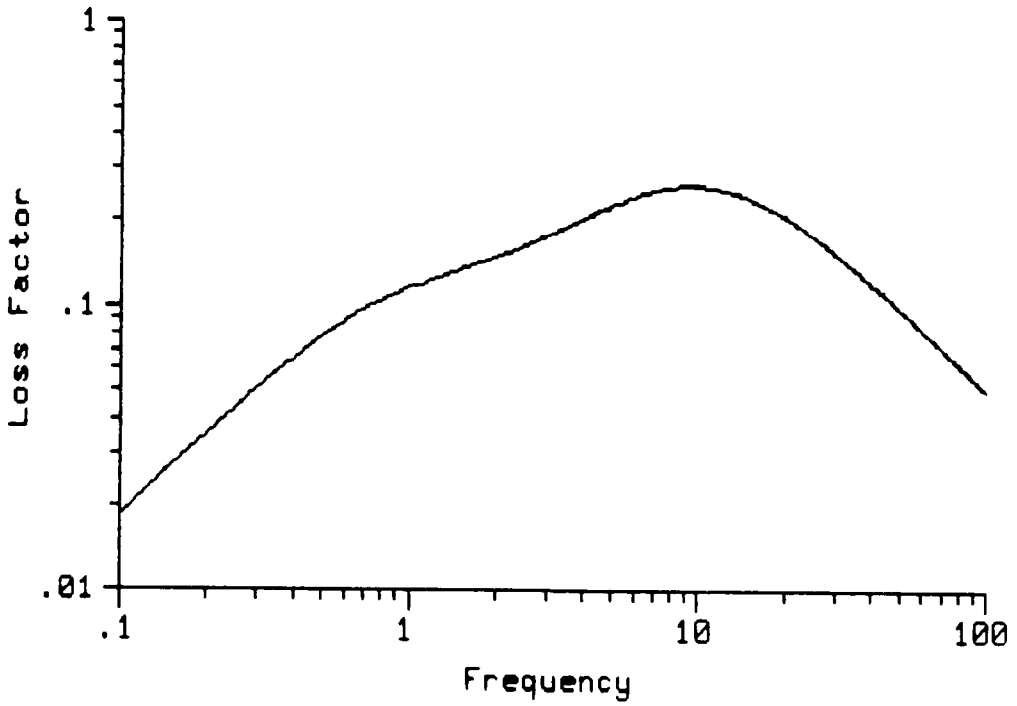

Figure 16. Two-ATF Model with Δ_2=0.5
(B_1=1, B_2=10, Δ_1=0.1, $\Delta_3=\sqrt{5}$ X 10^{-2})

is at the frequency corresponding to the value of B_i associated with the largest value, Δ_i.

As the strength of the coupling between the two ATFs is increased, the value of the loss factor at lower frequencies is increased. Figure 17 shows the plot of loss factor versus frequency for $\Delta_3 = \sqrt{40.5} \times 10^{-2}$, resulting from C^*=0.9. Again, a maximum at the value of frequency corresponding to B_2 is observed, but the lower maximum has shifted to the right and increased by an order of magnitude. A decrease in the value of Δ_3 does not, however, show the same trend, as is evidenced in figure 18. With an order of

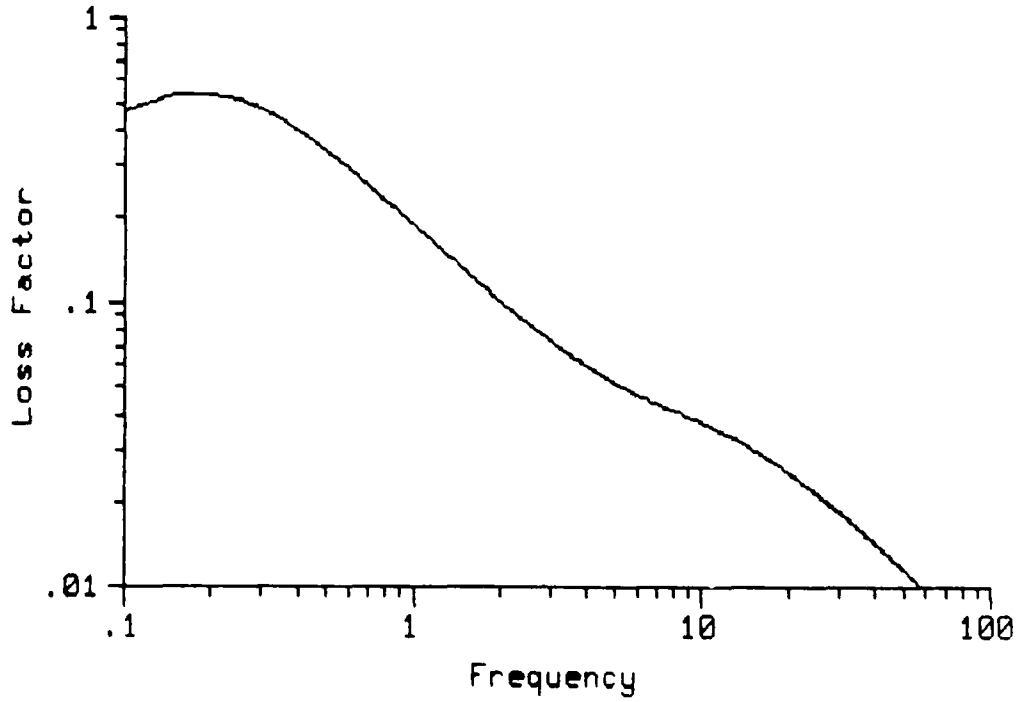

Figure 17. Two-ATF Model with $\Delta_3=\sqrt{40.5} \times 10^{-2}$ ($B_1=1$, $B_2=10$, $\Delta_1=0.1$, $\Delta_2=0.05$)

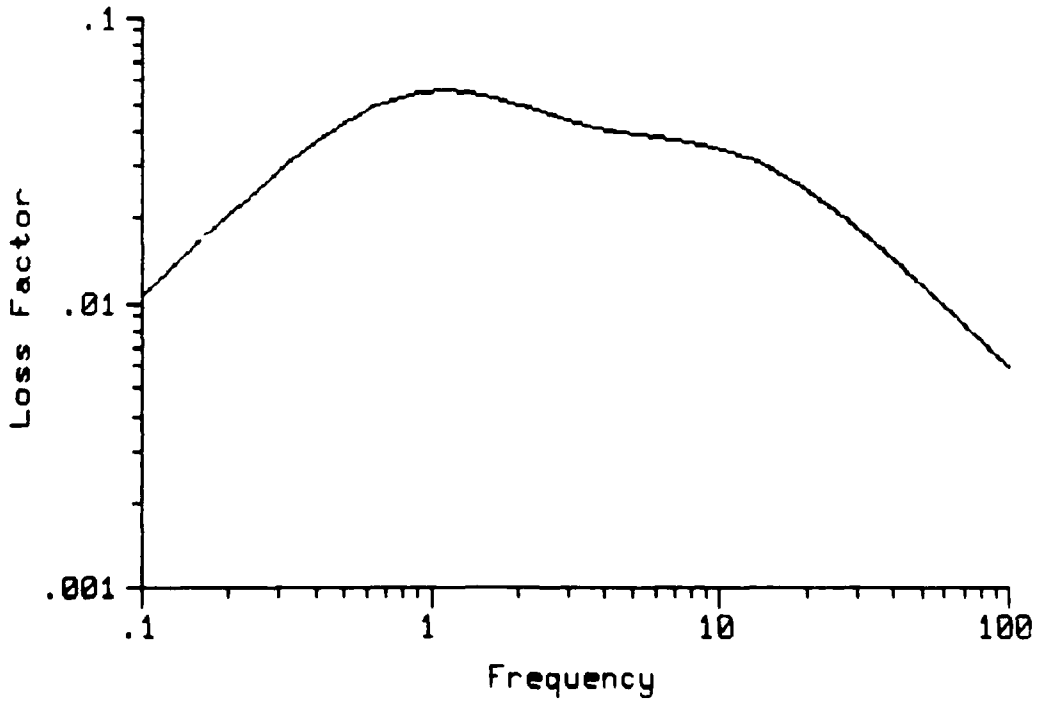

Figure 18. Two-ATF Model with $\Delta_3=\sqrt{0.5} \times 10^{-3}$ ($B_1=1$, $B_2=10$, $\Delta_1=0.1$, $\Delta_2=0.05$)

magnitude decrease in the value of C^* of equation (164) only a very slight decrease in the loss factor is noted.

Figure 19 shows a summary of the effects of varying the parameters of the two-ATF model. The arrow directions corresponds to the direction the curve will shift with an increase of the parameter shown.

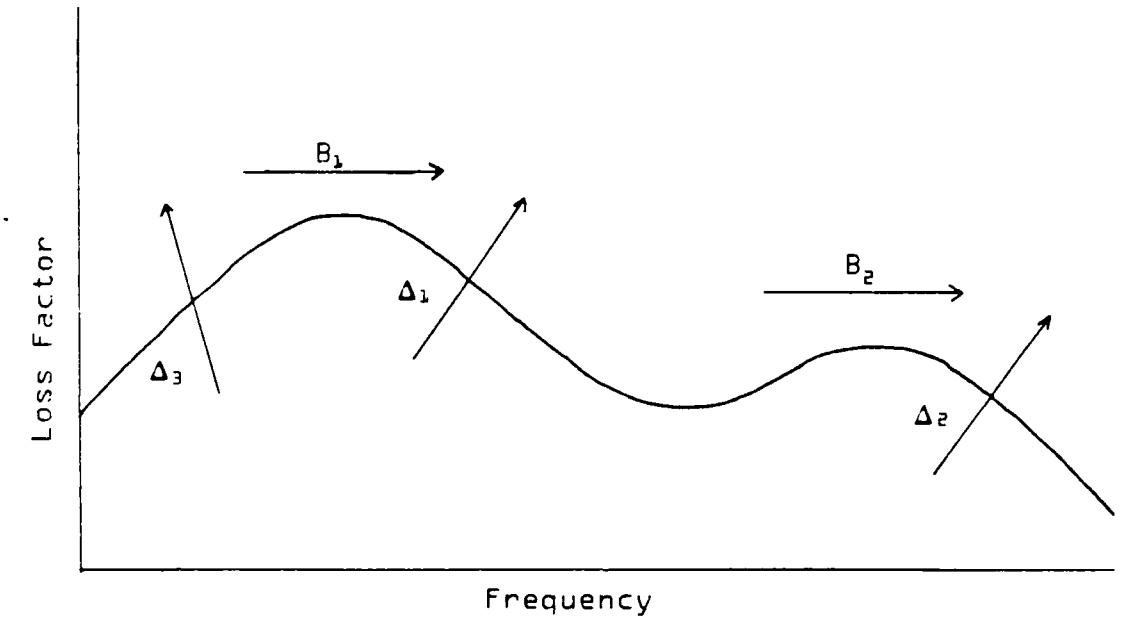

Figure 19 - Effect of Parameter Variation on Two-ATF Model

Two-ATF Model With Fractional Derivatives. A second augmenting thermodynamic field is now added to the model, and derivatives of fractional order are allowed in the time derivative terms of the thermodynamic equilibrium equations. The formulation of the problem follows the same path as previously; however, trigonometric relations are required

throughout the algebraic reduction in order to simplify the resulting equations for the complex modulus.

Constitutive Equations. The equation for the Helmholtz free energy used for the two-ATF model, equation (133), is used again:

$$f = 1/2E\epsilon^2 + 1/2\alpha_1\xi_1^2 + 1/2\alpha_2\xi_2^2 - \delta_1\epsilon\xi_1 - \delta_2\epsilon\xi_2 - \alpha_3\xi_1\xi_2 \quad (166)$$

Equation (134) is the equation of the stress field:

$$\sigma = \partial f/\partial\epsilon = E\epsilon - \delta_1\xi_1 + \delta_2\xi_2 \quad (167)$$

The affinities are given by equations (135) and (136):

$$A_1 = -\partial f/\partial\xi_1 = \delta_1\epsilon - \alpha_1\xi_1 + \alpha_3\xi_2 \quad (168)$$

$$A_2 = -\partial f/\partial\xi_2 = \delta_2\epsilon - \alpha_2\xi_2 + \alpha_3\xi_1 \quad (169)$$

Balancing the linear momentum equation gives

$$\partial\sigma/\partial x = \rho\ddot{u} = Eu'' - \delta_1\xi_1' + \delta_2\xi_2' \quad (170)$$

Recall from equation (137) that

$$\partial\xi_i/\partial t = -B_i(\xi_i - \bar{\xi}_i) \qquad i = 1,2 \quad (171)$$

Allowing fractional derivatives in the irreversible thermodynamic equilibrium equations of the time rate of change of ξ_1 and ξ_2, equations (141) and (142), results in the following:

$$\partial^q\xi_1/\partial t^q = -B_1\xi_1 + B_1\delta_1\epsilon/\alpha_1 + B_1\alpha_3\xi_2/\alpha_1 \quad (172)$$

$$\partial^r\xi_2/\partial t^r = -B_2\xi_2 + B_2\delta_2\epsilon/\alpha_2 + B_2\alpha_3\xi_1/\alpha_2 \quad (173)$$

Equations (172) and (173) together with equation (170) are the constitutive equations for a uniaxial rod modeled with two augmenting thermodynamic fields with general order derivatives. These equations are three partial differential

equations, coupled in u, ξ_1, and ξ_2, and can be solved more easily in the Fourier domain.

Damping Ratio. Taking the Fourier transform of equations (170), (172), and (173), with $i\omega$ introduced through the time derivatives and ik introduced through derivatives with respect to x, gives three equations which may be written in matrix form as

$$\begin{bmatrix} -\rho\omega^2 + Ek^2 & ik\delta_1 & ik\delta_2 \\ iB_1k\delta_1 & -\alpha_1[B_1+(i\omega)^q] & B_1\alpha_3 \\ iB_2k\delta_2 & B_2\alpha_3 & -\alpha_2[B_2+(i\omega)^r] \end{bmatrix} \begin{Bmatrix} U \\ Z_1 \\ Z_2 \end{Bmatrix} = \{\underline{0}\} \quad (174)$$

The determinant of the above matrix must equal zero in order to solve the linear system of equations which it represents. The determinant of equation (174) is then

$$\begin{aligned} &(-\rho\omega^2+Ek^2)\{(\alpha_1\alpha_2)[B_1+(i\omega)^q][B_2+(i\omega)^r] - B_1B_2\alpha_3^2\} \\ &- (ik\delta_1)\{(-\alpha_2)[iB_1k\delta_1][B_2+(i\omega)^r] - iB_1B_2k\alpha_3\delta_2\} \\ &+ (ik\delta_2)\{B_1B_2k\alpha_3\delta_1 - (-\alpha_1)[iB_2k\delta_2][B_1+(i\omega)^q]\}=0 \end{aligned} \quad (175)$$

After multiplication of terms inside the { } brackets, equation (175) can be written as

$$\begin{aligned} &(-\rho\omega^2+Ek^2)\{(\alpha_1\alpha_2)[B_1B_2+B_1(i\omega)^q+B_2(i\omega)^r+(i\omega)^{q+r}] \\ &\quad - B_1B_2\alpha_3^2\} - (k^2\delta_1)[B_1B_2\alpha_2\delta_1+B_1(i\omega)^r\alpha_2\delta_1 \\ &\quad +B_1B_2\alpha_3\delta_2] - (k^2\delta_2)[B_1B_2\alpha_3\delta_1+B_1B_2\alpha_1\delta_2 \\ &\quad +B_2(i\omega)^q\alpha_1\delta_2] = 0 \end{aligned} \quad (176)$$

Before solving this set of equations, the terms involving $(i\omega)^q$ and $(i\omega)^r$ must be written in a form that

allows for easier algebraic manipulation. Recall from the appendix that $i^q = \cos(q\pi/2) + i\sin(q\pi/2)$, and allow

$$q + r = s$$
$$q\pi/2 = x$$
$$r\pi/2 = y$$
$$s\pi/2 = z \tag{177}$$

Equation (176) may now be written in the following form:

$$\begin{aligned}(-\rho\omega^2+Ek^2)\{&\alpha_1\alpha_2[B_1B_2+B_1\omega^r\cos(y)+B_2\omega^q\cos(x)+\omega^s\cos(z)\\&+ i(B_1\omega^r\sin(y)+B_2\omega^q\sin(x)+\omega^s\sin(z))]-B_1B_2\alpha_3{}^3\}\\&- k^2[B_1B_2\alpha_3\delta_1\delta_2+B_1B_2\alpha_2\delta_1{}^2+B_1\omega^r\alpha_2\delta_1{}^2\cos(y)\\&+ iB_1\omega^r\alpha_2\delta_1{}^2\sin(y)] - k^2[B_1B_2\alpha_3\delta_1\delta_2+B_1B_2\alpha_1\delta_2{}^2\\&+ B_2\omega^q\alpha_1\delta_2{}^2\cos(x)-iB_2\omega^q\alpha_1\delta_2{}^2\sin(x)] = 0\end{aligned} \tag{178}$$

Dividing this equation by the term which multiplies $(-\rho\omega^2 + Ek^2)$ results in an equation of the form

$$-\rho\omega^2 + Ek^2 - k^2(N_1/D_1) = 0 \tag{179}$$

where

$$\begin{aligned}N_1 = {}&2B_1B_2\alpha_3\delta_1\delta_2 + B_1B_2\alpha_2\delta_1{}^2 + B_1B_2\alpha_1\delta_2{}^2\\&+ B_1\omega^r\alpha_2\delta_1{}^2\cos(y) + B_2\omega^q\alpha_1\delta_2{}^2\cos(x)\\&+ i[B_1\omega^r\alpha_2\delta_1{}^2\sin(y) + B_2\omega^q\alpha_1\delta_2{}^2\sin(x)]\end{aligned} \tag{180}$$

and

$$\begin{aligned}D_1 = {}&B_1B_2(\alpha_1\alpha_2 - \alpha_3{}^2) + \alpha_1\alpha_2[B_1\omega^r\cos(y) + B_2\omega^q\cos(x)\\&+ \omega^s\cos(z)] + i\alpha_1\alpha_2[B_1\omega^r\sin(y) + B_2\omega^q\sin(x)\\&+ \omega^s\sin(x)]\end{aligned} \tag{181}$$

Factoring $EB_1B_2\alpha_1\alpha_2$ from the numerator, N_1, and recalling the definitions of Δ_1, Δ_2, and Δ_3 from equation (150) results in

$$N_1 = EB_1B_2\alpha_1\alpha_2\{\Delta_3 + \Delta_1[1 + (\omega^r/B_2)\cos(y)]$$
$$+ \Delta_2[1 + (\omega^q/B_1)\cos(x)] + i[(\Delta_1\omega^r/B_2)\sin(y)$$
$$+ (\Delta_2\omega^q/B_1)\sin(x)]\} \quad (182)$$

Factoring $B_1B_2\alpha_1\alpha_2$ from the denominator, D_1, and recalling that $\gamma = 1 - \alpha_3^2/(\alpha_1\alpha_2)$ gives

$$D_1 = B_1B_2\alpha_1\alpha_2\{\gamma + (\omega^q/B_1)\cos(x) + (\omega^r/B_2)\cos(y)$$
$$+ (\omega^s/B_1B_2)\cos(z) + i[(\omega^q/B_1)\sin(x) + (\omega^r/B_2)\sin(y)$$
$$+ (\omega^s/B_1B_2)\sin(z)]\} \quad (183)$$

Dividing equation (179) by ρ and rearranging, with the $EB_1B_2\alpha_1\alpha_2$ canceling, leaves an equation from which the complex modulus can be extracted:

$$-\omega^2 + E(k^2/\rho)[1 - N_2/D_2] = 0 \quad (184)$$

where N_2 and D_2 are defined by equations (182) and (183) divided by $B_1B_2\alpha_1\alpha_2$, repectively. The equation inside the [ ] brackets is the complex modulus divided by E, and the loss factor can be derived from equation (4). To do this, however, both N_2 and D_2 must be multiplied by the complex conjugate of D_2:

$$\overline{D_2} = \gamma + (\omega^q/B_1)\cos(x) + (\omega^r/B_2)\cos(y)$$
$$+ (\omega^s/B_1B_2)\cos(z) - i\,[(\omega^q/B_1)\sin(x)$$
$$+ (\omega^r/B_2)\sin(y) + (\omega^s/B_1B_2)\sin(z)] \quad (185)$$

In order to simplify the resulting equations three trigonometric relations were required:

$$\sin(x \pm y) = \sin(x)\cos(y) \pm \cos(x)\sin(y)$$
$$\cos(x \pm y) = \cos(x)\cos(y) \mp \sin(x)\sin(y)$$
$$A = A\sin^2(x) + A\cos^2(x) \quad (186)$$

Following extensive algebraic manipulation and employing the above trigonometric relations results in the following expressions for the numerator, N_2, and the denominator, D_2, of equation (184):

$$
\begin{aligned}
N_1\,(1/E) = {} & \Delta_1\,[\gamma + (\omega^r/B_2)^2 + (\omega^q/B_1)\cos(x) \\
& + (\gamma + 1)(\omega^r/B_2)\cos(y) + (\omega^s/B_1B_2)\cos(z) \\
& + (\omega^s/B_1B_2)\cos(x-y) + (\omega^{(r+s)}/B_1B_2^2)\cos(z-y)] \\
& + \Delta_2\,[\gamma + (\omega^q/B_1)^2 + (\gamma + 1)(\omega^q/B_1)\cos(x) \\
& + (\omega^r/B_2)\cos(y) + (\omega^s/B_1B_2)\cos(z) \\
& + (\omega^s/B_1B_2)\cos(x-y) + (\omega^{(q+s)}/B_1^2B_2)\cos(z-x)] \\
& + \Delta_3\,[\gamma + (\omega^q/B_1)\cos(x) + (\omega^r/B_2)\cos(y) \\
& + (\omega^s/B_1B_2)\cos(z)] \\
& + i\,\{\Delta_1\,[-(\omega^q/B_1)\sin(x) + (\gamma - 1)(\omega^r/B_2)\sin(y) \\
& - (\omega^s/B_1B_2)\sin(z) + (\omega^s/B_1B_2)\sin(y-x) \\
& + (\omega^{(r+s)}/B_1B_2^2)\sin(y-z)] \\
& + \Delta_2\,[(\gamma - 1)(\omega^q/B_1)\sin(x) - (\omega^r/B_2)\sin(y) \\
& - (\omega^s/B_1B_2)\sin(z) + (\omega^s/B_1B_2)\sin(x-y) \\
& + (\omega^{(q+s)}/B_1^2B_2)\sin(x-z)] \\
& - \Delta_3\,[(\omega^q/B_1)\sin(x) + (\omega^r/B_2)\sin(y) \\
& + (\omega^s/B_1B_2)\sin(z)]\} \qquad (187)
\end{aligned}
$$

$$
\begin{aligned}
D_2 = {} & \gamma^2 + 2\gamma[(\omega^q/B_1)\cos(x) + (\omega^r/B_2)\cos(y) \\
& + (\omega^s/B_1B_2)\cos(z)] + (\omega^q/B_1)^2 + (\omega^r/B_2)^2 + (\omega^s/B_1B_2)^2 \\
& + (2\omega^s/B_1B_2)\,[\cos(x-y) + (\omega^q/B_1)\cos(z-x) \\
& + (\omega^r/B_2)\cos(y-z)] \qquad (188)
\end{aligned}
$$

The loss factor becomes

$$\eta = Im[E^*(\omega)]/Re[E^*(\omega)]$$

$$= (Im[D_2-N_2]/D_2)/(Re[D_2-N_2]/D_2) \qquad (189)$$

Again, the assumptions of small damping and $\Delta_1 << 1$, $\Delta_2 << 1$, and $\Delta_3 << 1$, leading to equation (156) are made here. Two other relationships help further reduce the resulting loss factor. Recalling the definitions of x, y, and z given in equation (177), gives the following relationships:

$$z - y = (q+r)(\pi/2) - r\pi/2 = q\pi/2 = x$$

$$z - x = (q+r)(\pi/2) - q\pi/2 = r\pi/2 = y \qquad (190)$$

Using trigonometric relationships for the sine and cosine functions results in

$$\sin(x-z) = -\sin(z-x) = -\sin(y)$$

$$\sin(y-z) = -\sin(z-y) = -\sin(x)$$

$$\cos(x-z) = \cos(z-x) = \cos(y)$$

$$\cos(y-z) = \cos(z-y) = \cos(x) \qquad (191)$$

The loss factor then becomes

$$\eta = N_{loss}/D_{loss} \qquad (192)$$

where

$$N_{loss} = \Delta_1 \{[(\omega^q/B_1) + (\omega^{(r+s)}/B_1B_2^2)]\sin(x)$$
$$+ (\omega^s/B_1B_2)[\sin(z) + \sin(x-y)]$$
$$+ (1-\gamma)(\omega^r/B_2)\sin(y)\} + \Delta_2 \{[(1-\gamma)(\omega^q/B_1)\sin(x)$$
$$+ [(\omega^r/B_2) + (\omega^{(q+s)}/B_1^2B_2)]\sin(y)$$
$$+ (\omega^s/B_1B_2)[\sin(z) + \sin(y-x)]\}$$
$$+ \Delta_3 [(\omega^q/B_1)\sin(x) + (\omega^r/B_2)\sin(y)$$
$$+ (\omega^s/B_1B_2)\sin(z)] \qquad (193)$$

and

$$D_{loss} = \gamma^2 + 2\gamma[(\omega^q/B_1)\cos(x) + (\omega^r/B_2)\cos(y) + (\omega^s/B_1B_2)\cos(z)] + (\omega^q/B_1)^2 + (\omega^r/B_2)^2 + (\omega^s/B_1B_2)^2 + (2\omega^s/B_1B_2)[\cos(x-y) + (\omega^q/B_1)\cos(y) + (\omega^r/B_2)\cos(x)] \quad (194)$$

With the assumption of small damping, the damping ratio is equal to half the loss factor.

As an added check on the algebra, the loss factor of the two-ATF model with fractional derivatives, equation (192), should reduce to the loss factor of the single-ATF model with fractional derivatives, twice equation (116), in the same manner equation (156) reduced to equation (41) when the two-ATF model without fractional derivatives was compared to the single-ATF model. Setting $\alpha_3 = \delta_2 = 0$, which in turn drives $\Delta_2 = \Delta_3 = 0$ and $\gamma = 1$, in equation (192), then multiplying the numerator and denominator by B_2^2 results in the following:

$$\eta = N_{ck}/D_{ck} \quad (195)$$

where

$$N_{ck} = \Delta_1 \{B_2^2(\omega^q/B_1)\sin(x) + B_2(\omega^s/B_1)[\sin(z) + \sin(x-y) + \omega^r\sin(x)]\} \quad (196)$$

and

$$D_{ck} = B_2^2 [1 + 2(\omega^q/B_1)\cos(x) + (\omega^q/B_1)^2] + B_2 [2\omega^r\cos(y) + 2(\omega^s/B_1)\cos(z) + 2(\omega^s/B_1)\cos(x-y) + 2(\omega^{(q+s)}/B_1^2)\cos(y)] + 2(\omega^{(r+s)}/B_1)\cos(x) + (\omega^r)^2 + (\omega^s/B_1)^2 \quad (197)$$

Taking the limit of equation (195) as B_2 goes to infinity results in an indeterminant form. L'Hospital's rule is invoked twice, and the resulting limit gives

$$\eta = \frac{\Delta_1(\omega^q/B_1)\sin(x)}{1 + (2\omega^q/B_1)\cos(x) + (\omega^q/B_1)^2} \qquad (198)$$

which exactly equals twice equation (114), and the loss factor, therefore, reduces to that of the single-ATF fractional derivative model.

Characteristics of the Two-ATF Model With Fractional Derivatives. Figure 20 is a plot of the loss factor versus frequency for the two-ATF model with the values of the parameters as follows:

$q = 0.8$	$B_1 = 1$	$\Delta_1 = 0.1$
$r = 0.4$	$B_2 = 50$	$\Delta_2 = 0.05$
		$\Delta_3 = 5 \times 10^{-2}$

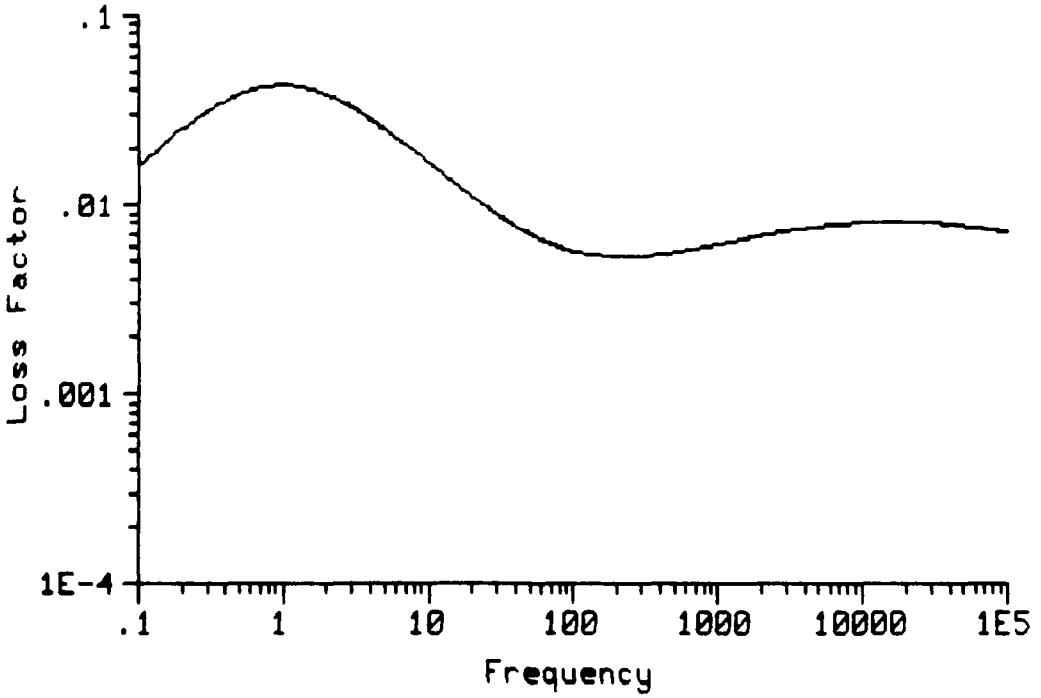

Figure 20. Loss Factor vs. Frequency for the Two-ATF Model with Fractional Derivatives

Figure 20 shows a similar "double hump" characteristic to that of the two-ATF model without fractional derivatives. The first maximum falls under the value of frequency corresponding to the value of B_1. However, unlike the two-ATF model without fractional derivatives, the second maximum would appear not to correspond to B_2. Comparing equation (192) to equation (156) shows that the B_i of equation (156) are raised to the same power as ω. In equation (192), however, this is not the case. To find the value of frequency at which the maxima for the loss factor corresponding the two-ATF model with fractional derivatives will occur, the values of the B_i must be raised to the power of inverse of the respective fraction to which the corresponding ω is raised. For example,

$$B_1 = 1, \quad q = 0.8$$

$$\Longrightarrow \omega = (1)^{(1/0.8)} = (1)^{1.25} = 1 \qquad (199)$$

which is the value of frequency corresponding to the first maximum. Likewise, for

$$B_2 = 50, \quad r = 0.4$$

$$\Longrightarrow \omega = (50)^{(1/0.4)} = (50)^{2.5} = 17678 \qquad (200$$

Again, the value corresponds to the frequency of the second maximum in figure 20.

Notice also that the slopes of the two portions of the curve are different, with the slopes of the first maximum being greater than those of the second maximum.

Equations (166), (172), and (173) are symmetric with respect to the two ATFs, as well as the other material constants. This fact leads to the conclusion that the loss factor must also be symmetric with respect to the parameters of the model. Exchanging the values of all parameters with subscript 1 for those with subscript 2, e.g., $B_1 = B_2$ and $B_2 = B_1$, as well as exchanging the values of the fractional powers, q and r, results in a plot of the loss factor that is exactly the same as figure 20. This, then, is an added check on the algebra performed to arrive at equation (192).

Figures 21 through 34 show the loss factor versus frequency as various parameters of the two-ATF model with fractional derivatives are varied.

The value of q is reduced to 0.1 in figure 21. The first maximum is no longer visible, and the value of the second maximum has increased. When q is increased to 0.95 in figure 22, the value of the peak is increased, while the maximum of the second peak remains the same. The slope of the first "hump" or curve is clearly greater as well, as is evidenced by the narrowing of the peak, and the deepening of the minimum as the first curve leads into the second curve.

Values of r are varied in figures 23 and 24. First, r is reduced to 0.1, and the second peak shifts to the right. The maximum value of the first peak remains unchanged. As r is increased to 0.85, the second peak shifts towards the

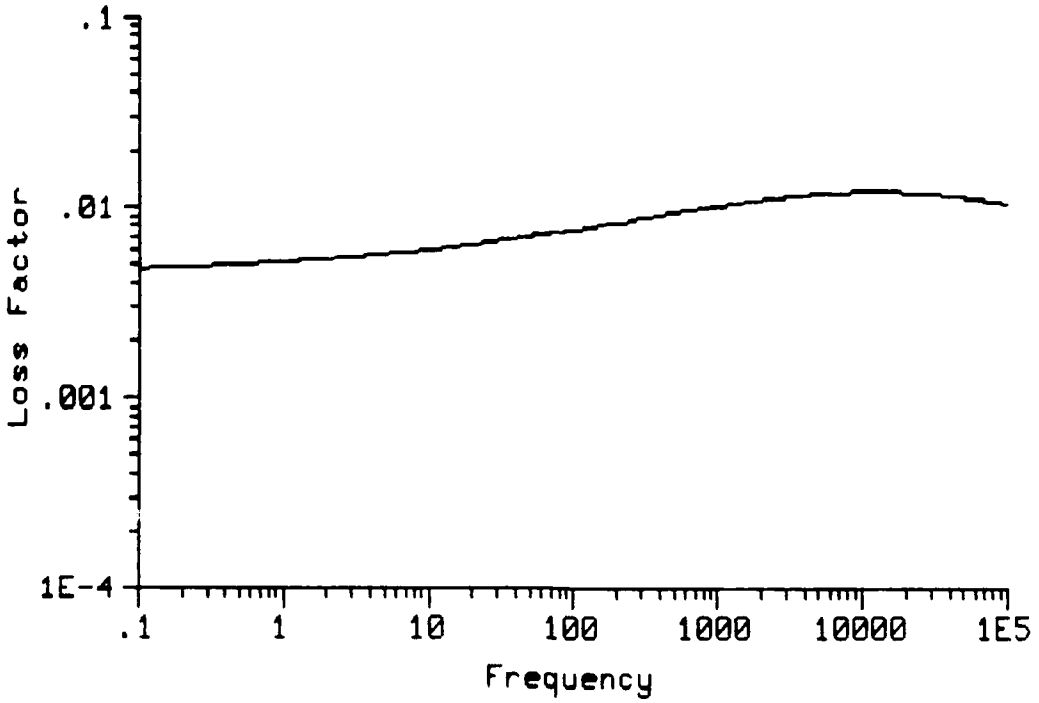

Figure 21. Fractional Derivative 2-ATF Model with q=0.1 ($r=0.4$, $B_1=1$, $B_2=50$, $\Delta_1=-0.1$, $\Delta_2=0.05$, $\Delta_3=\sqrt{5}$ X 10^{-2})

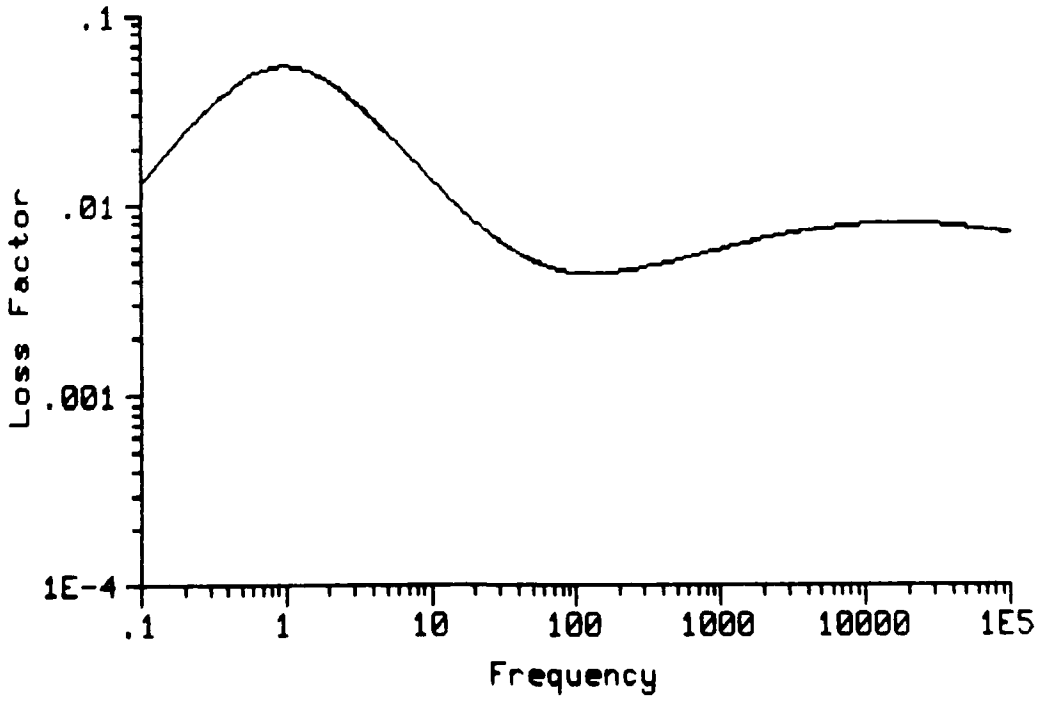

Figure 22. Fractional Derivative 2-ATF Model with q=0.95 ($r=0.4$, $B_1=1$, $B_2=50$, $\Delta_1=0.1$, $\Delta_2=0.05$, $\Delta_3=\sqrt{5}$ X 10^{-2})

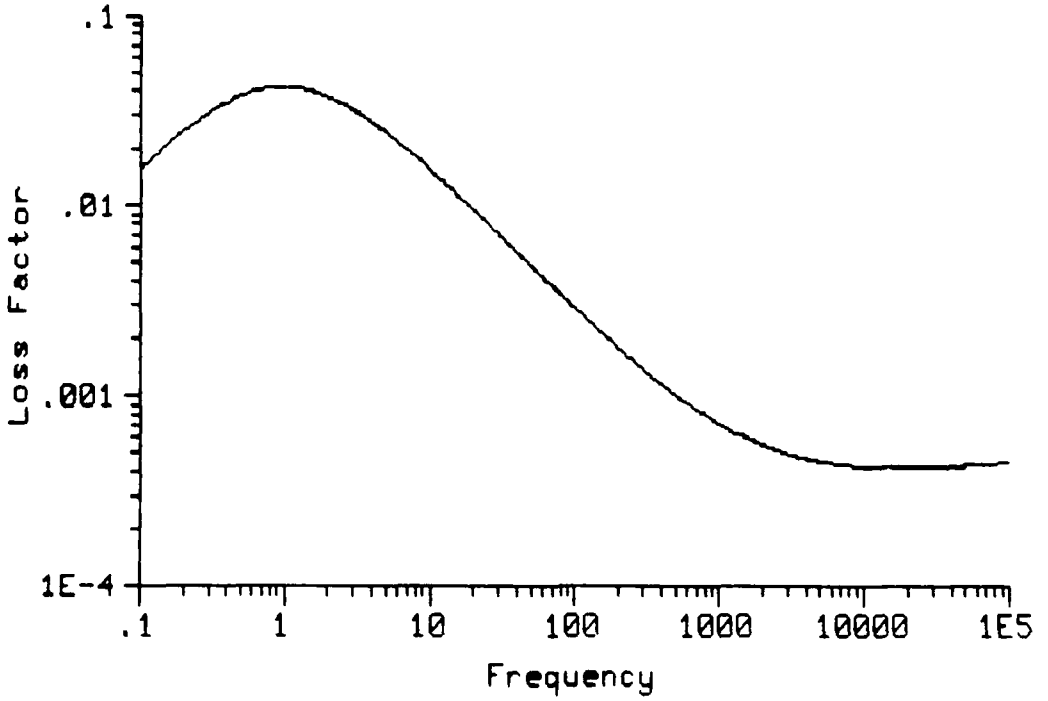

Figure 23. Fractional Derivative 2-ATF Model with r=0.1
($q=0.8$, $B_1=1$, $B_2=50$, $\Delta_1=0.1$, $\Delta_2=0.05$, $\Delta_3=\sqrt{5} \times 10^{-2}$)

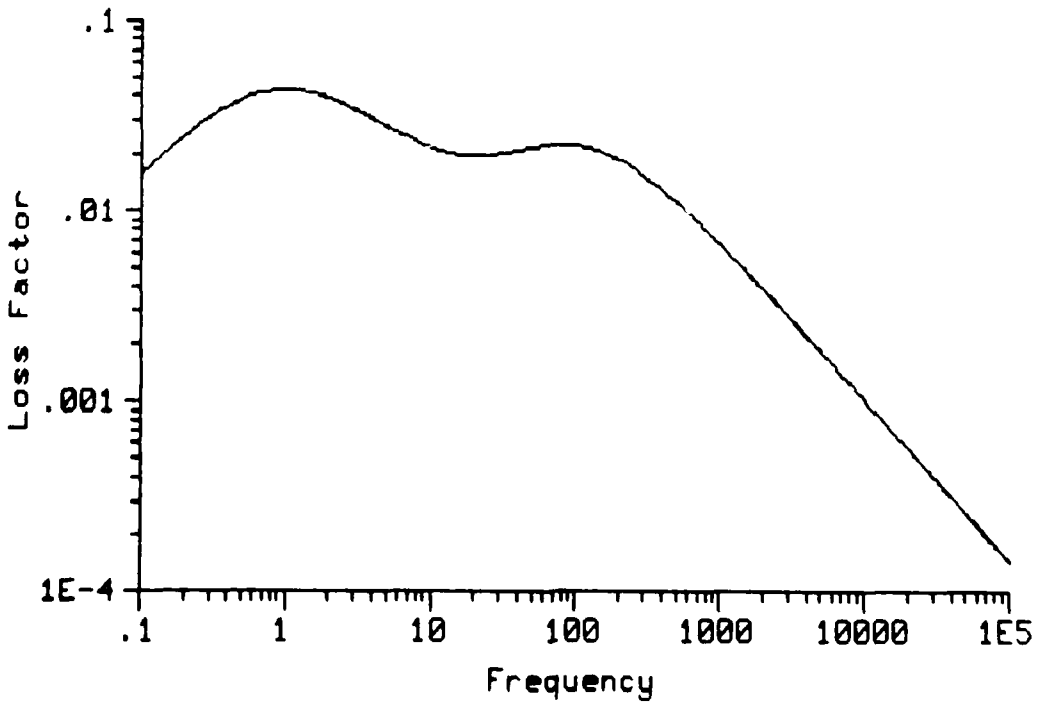

Figure 24. Fractional Derivative 2-ATF Model with r=0.85
($q=0.8$, $B_1=1$, $B_2=50$, $\Delta_1=0.1$, $\Delta_2=0.05$, $\Delta_3=\sqrt{5} \times 10^{-2}$)

first peak on the left, and the value of the second maximum increases. Once again, the value of the first maximum remains constant. It will also be noted that the value of the slope of the second curve has increased as well.

Figure 25 shows the plot of the loss factor versus frequency when B_1 is decreased to 0.3. The peak now corresponds to a frequency of 0.22 ($\omega = (0.3)^{1.25}$), with the slopes and maximum the same as originally plotted -- the first maximum has just shifted to the left. The second peak

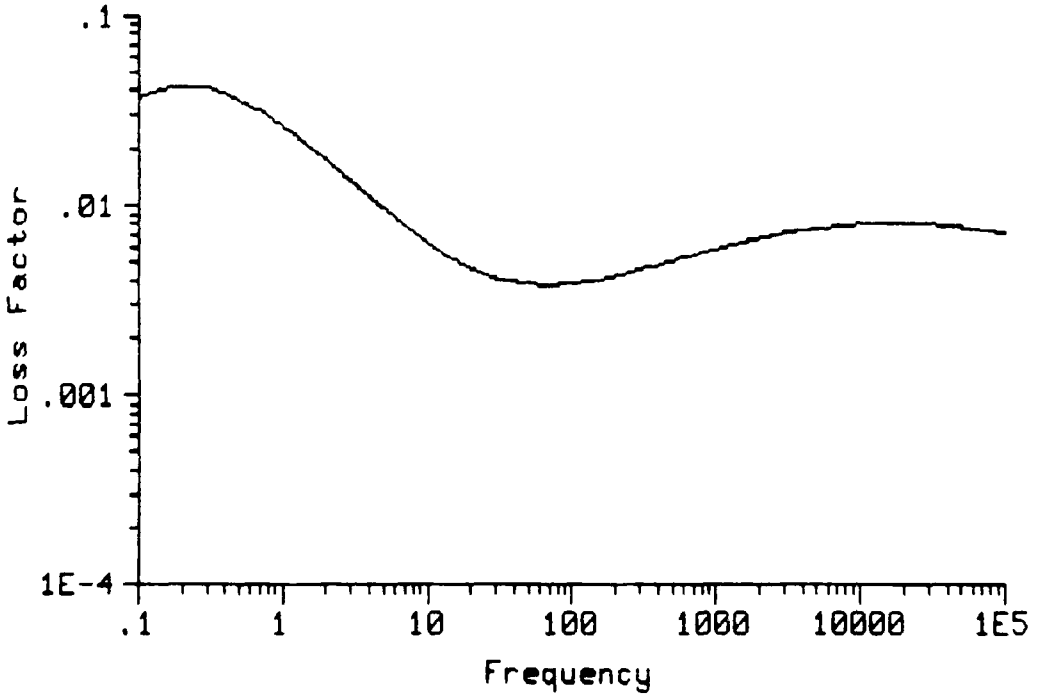

Figure 25. Fractional Derivative 2-ATF Model with B_1=0.3 (q=0.8, r=0.4, B_2=50, Δ_1=0.1, Δ_2=0.05, $\Delta_3=\sqrt{5} \times 10^{-2}$)

is now also more clearly discernable. When B_1 is increased to 30 in figure 26 the curve shifts to the right with the maximum corresponding to a frequency of 70. The second

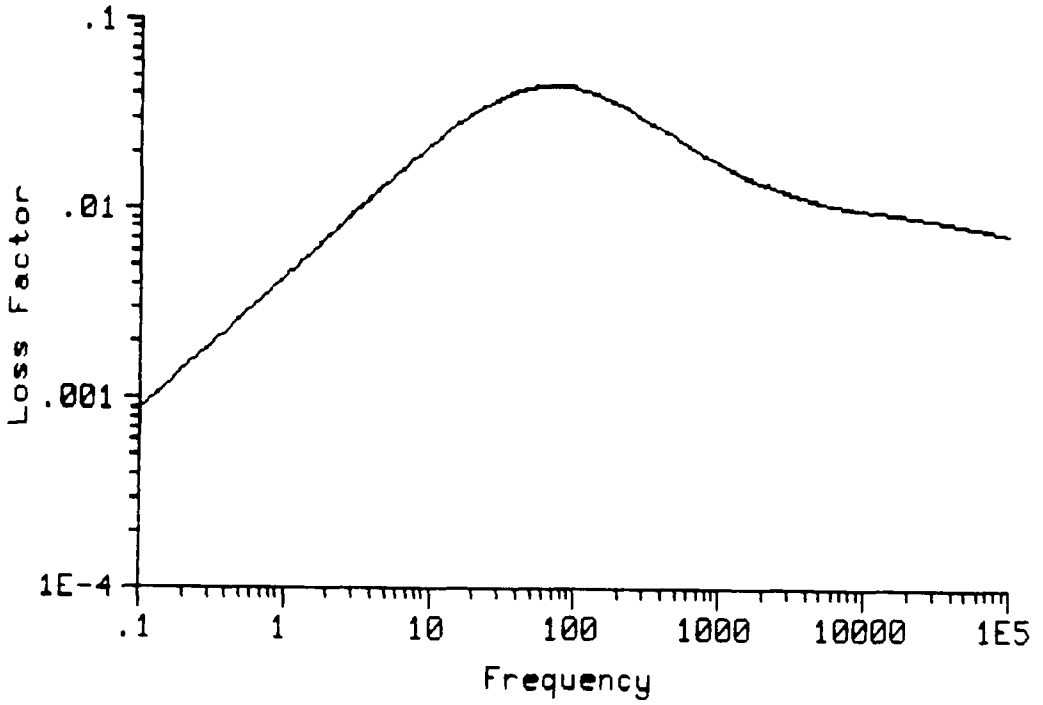

Figure 26. Fractional Derivative 2-ATF Model with B_1=30 (q=0.8, r=0.4, B_2=50, Δ_1=0.1, Δ_2=0.05, $\Delta_3=\sqrt{5} \times 10^{-2}$)

maximum is now almost a part of the first curve, but can still be seen as an inflection point.

With B_2 reduced to 5 in figure 27 the plot of loss factor versus frequency shows the shift of the second maximum to the left, with the maximum now an inflection point on the curve at a frequency of 56. The slope following the inflection point clearly differs from the slope preceeding the point, showing the slope dependence on the fractional powers of the model. Likewise, as the value of B_2 is increased to 1000 in figure 28, the maximum of the second curve shifts to the right. The maximum should correspond to a frequency of 3×10^7.

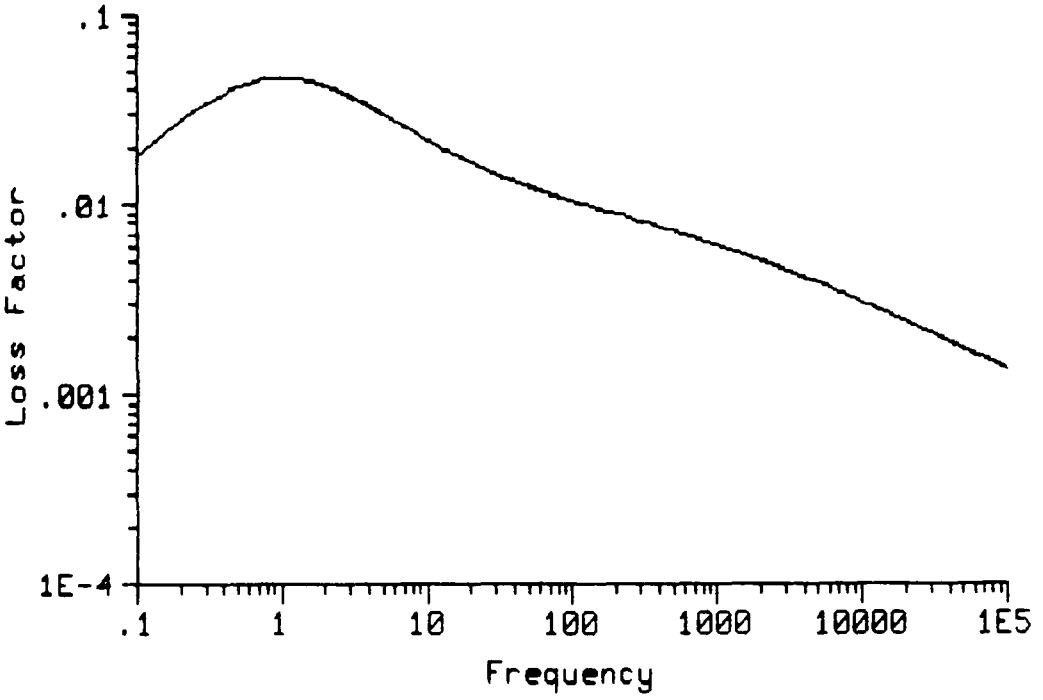

Figure 27. Fractional Derivative 2-ATF Model with B_2=5 (q=0.8, r=0.4, B_1=1, Δ_1=0.1, Δ_2=0.05, $\Delta_3=\sqrt{5}$ X 10^{-2})

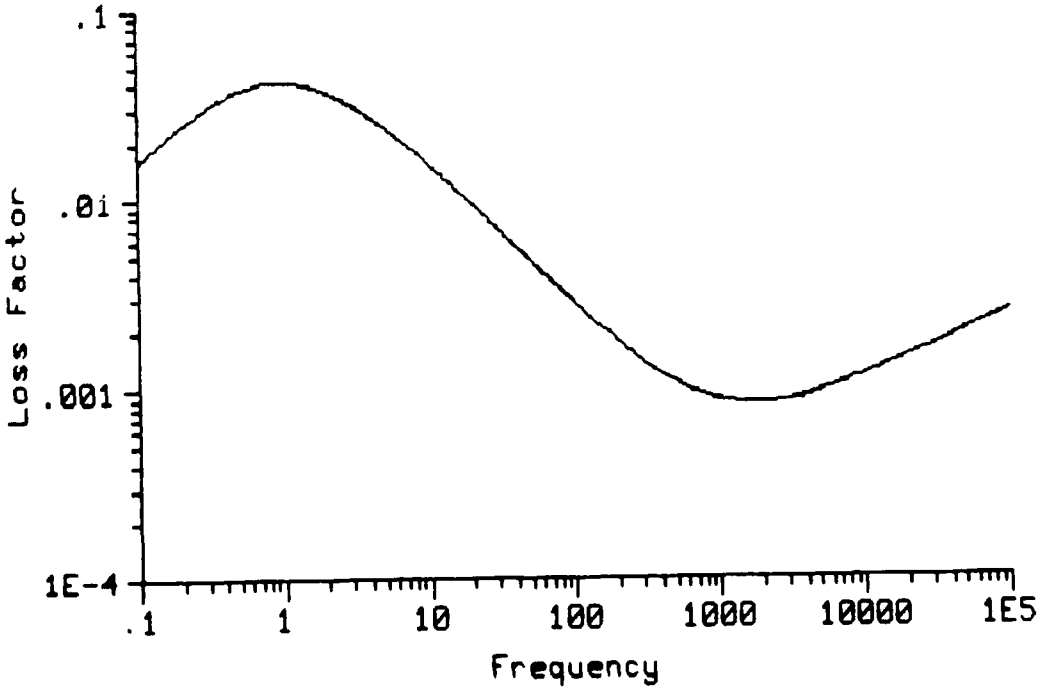

Figure 28. Fractional Derivative 2-ATF Model with B_2=1000 (q=0.8, r=0.4, B_1=1, Δ_1=0.1, Δ_2=0.05, $\Delta_3=\sqrt{5}$ X 10^{-2})

The value of Δ_1 affects the value of the maximum of the first peak, as can be seen in figures 29 and 30. Reducing Δ_1 to 0.01, and order of magnitude, reduces the maximum by almost an order of magnitude in figure 29. Increasing the value of Δ_1 has the opposite effect of increasing the magnitude of the peak in figure 30. In both cases, however, the value of the second maximum remains unaffected.

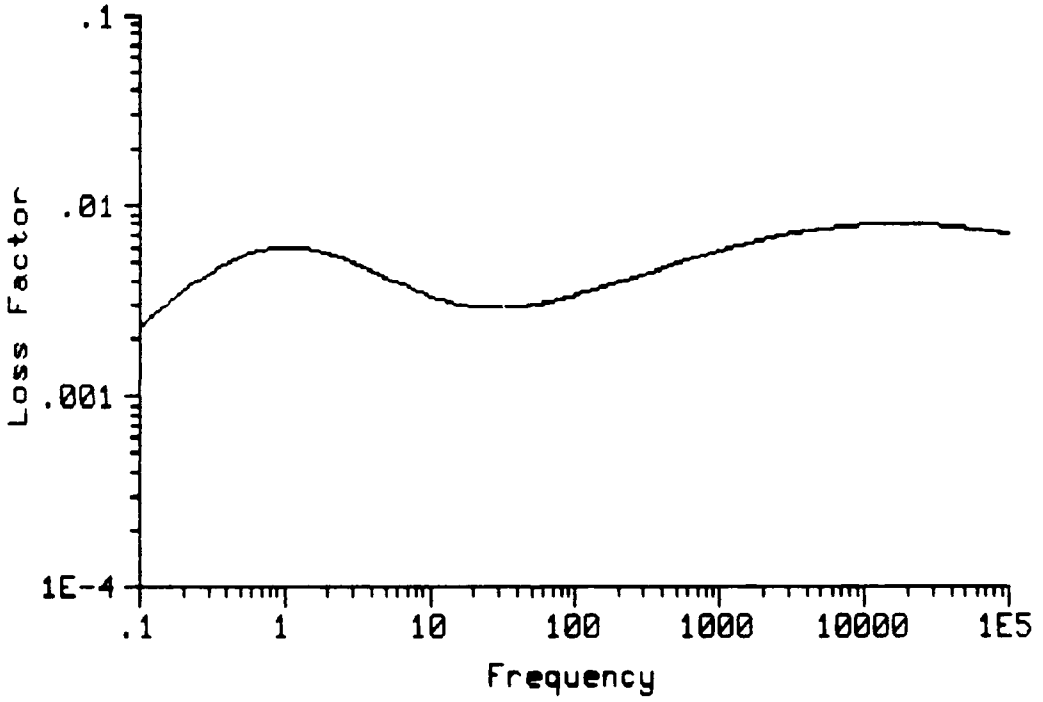

Figure 29. Fractional Derivative 2-ATF Model with Δ_1=0.01 (q=0.8, r=0.4, B_1=1, B_2=50, Δ_2=0.05, $\Delta_3=\sqrt{5}$ X 10^{-2})

Figures 31 and 32 show the effects of varying Δ_2. If Δ_2 is decreased as in figure 31, the value of the second peak's magnitude decreases accordingly. Increasing Δ_2 to 0.5 in figure 32 increases not only the magnitude of the second peak quite drastically, but also that of the first peak, although to a much weaker extent.

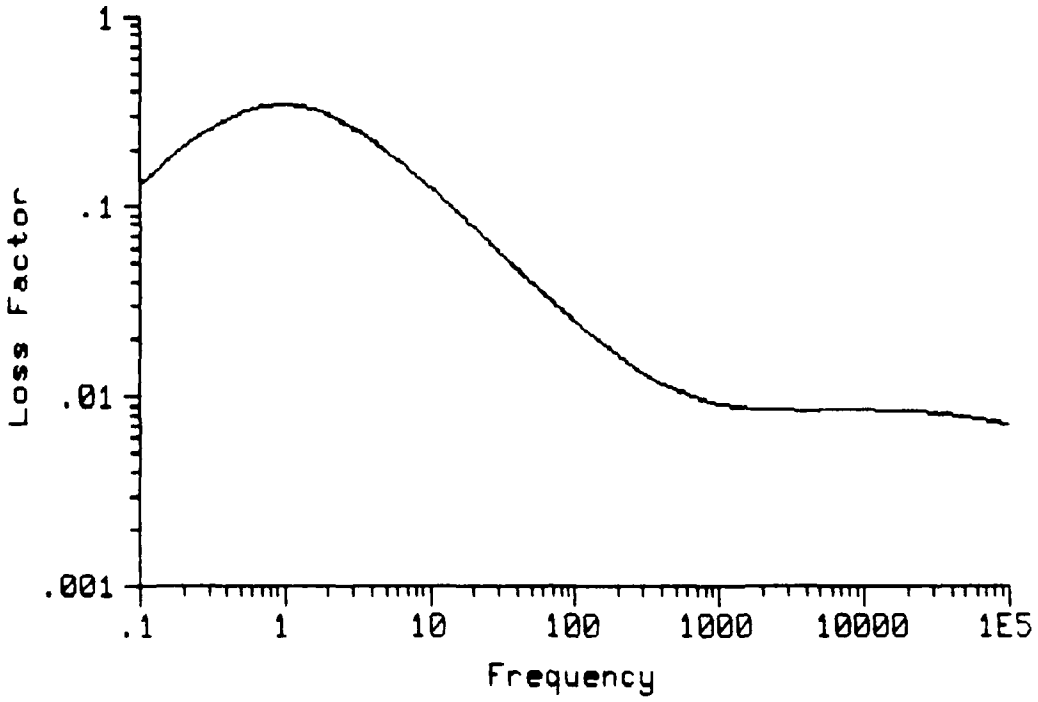

Figure 30. Fractional Derivative 2-ATF Model with Δ_1=0.9 (q=0.8, r=0.4, B_1=1, B_2=50, Δ_2=0.05, $\Delta_3=\sqrt{5}$ X 10^{-2})

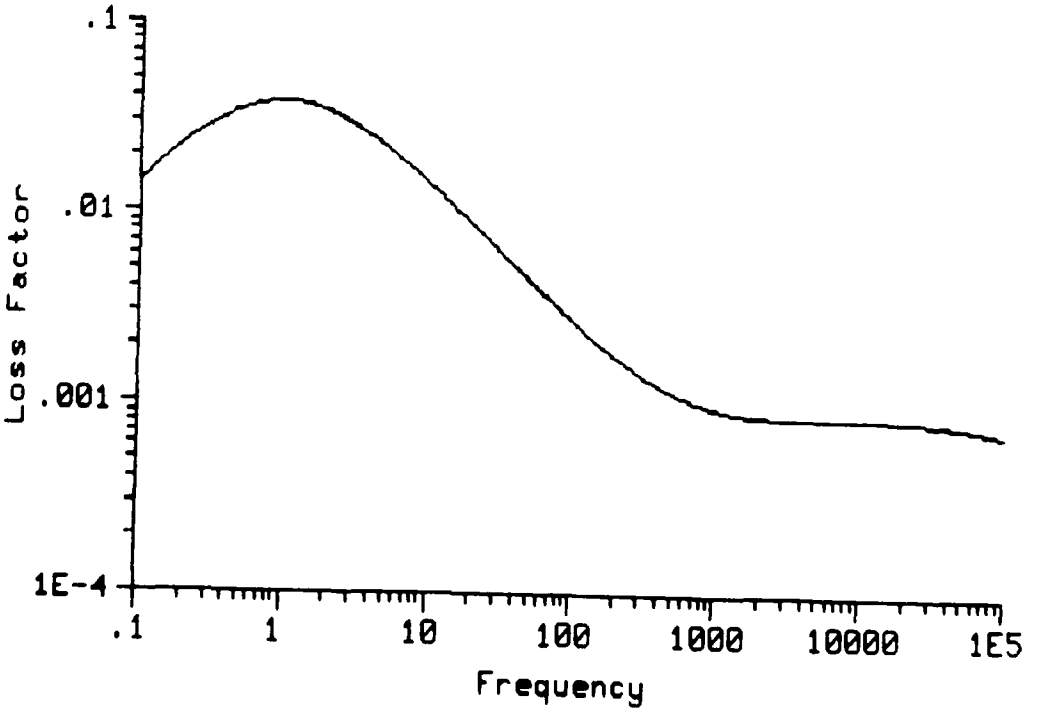

Figure 31. Fractional Derivative 2-ATF Model with Δ_2=0.005 (q=0.8, r=0.4, B_1=1, B_2=50, Δ_1=0.1, $\Delta_3=\sqrt{5}$ X 10^{-2})

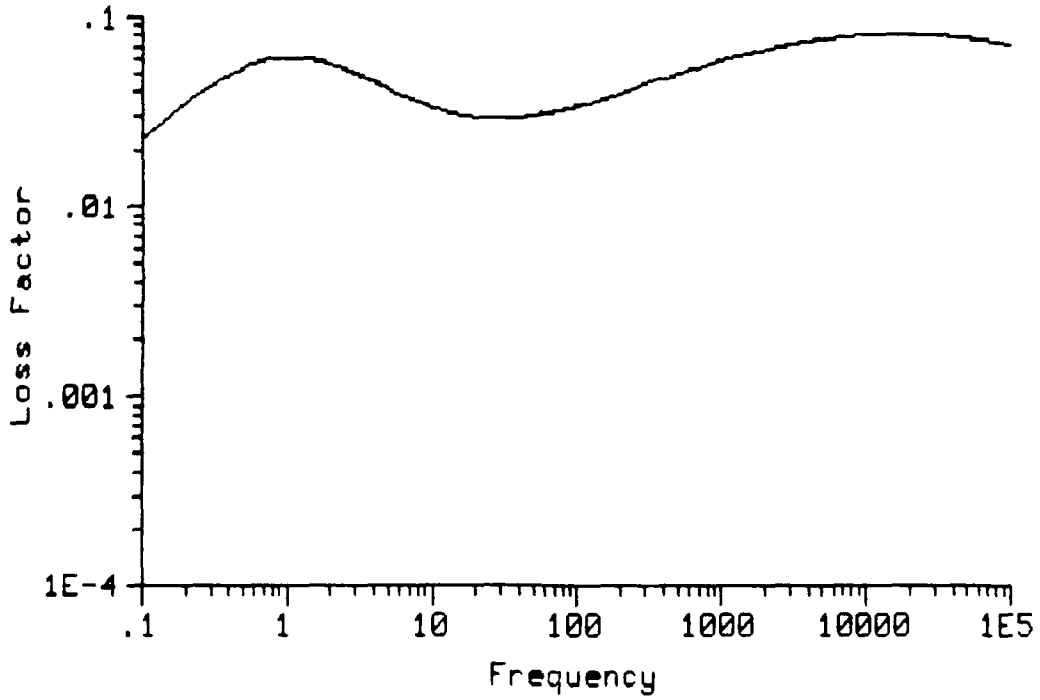

Figure 32. Fractional Derivative 2-ATF Model with Δ_2=0.5 (q=0.8, r=0.4, B_1=1, B_2=50, Δ_1=0.1, $\Delta_3=\sqrt{5}$ X 10^{-2})

Finally, the value of Δ_3 is varied in figures 33 and 34. Reducing Δ_3 to $\sqrt{0.5}$ X 10^{-3} by reducing C' an order of magnitude does little to the overall curve except for reducing the value of the magnitude of the first peak only slightly. Increasing Δ_3 to $\sqrt{40.5}$ X 10^{-2} by increasing C' to 0.9, however, increases the value of the first peak by an order of magnitude, and shifts it to the left. The second peak, in turn, is only affected slightly, with a small increase in the magnitude visible.

The effects of variations in the model paramaters are summarized in figure 35. Increasing the parameter will shift the curve in the direction shown.

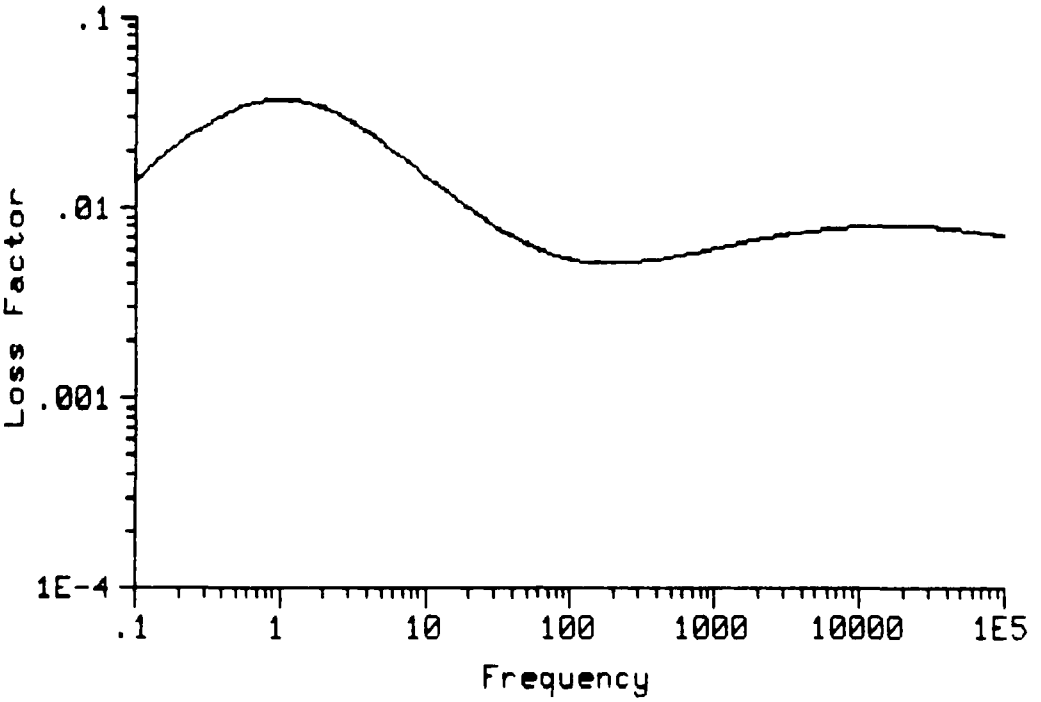

Figure 33. Two-ATF Fractional Derivative Model with $\Delta_3=\sqrt{0.5}$ X 10^{-3}
(q=0.8, r=0.4, B_1=1, B_2=50, Δ_1=0.1, Δ_2=0.05)

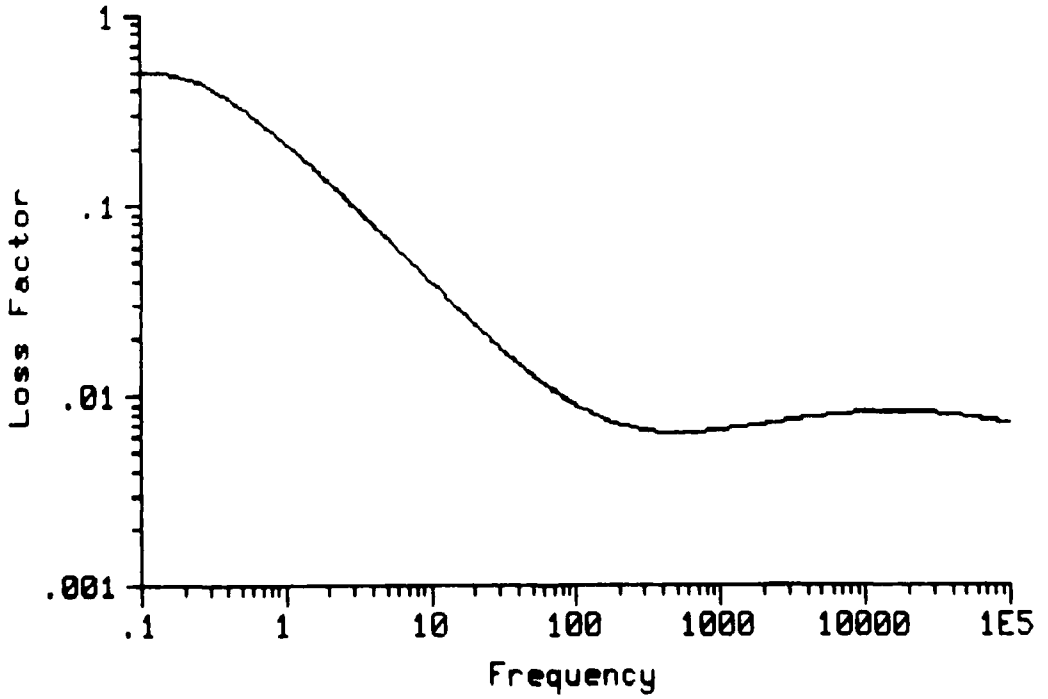

Figure 34. Two-ATF Fractional Derivative Model with $\Delta_3=\sqrt{40.5}$ X 10^{-2}
(q=0.8, r=0.4, B_1=1, B_2=50, Δ_1=0.1, Δ_2=0.05)

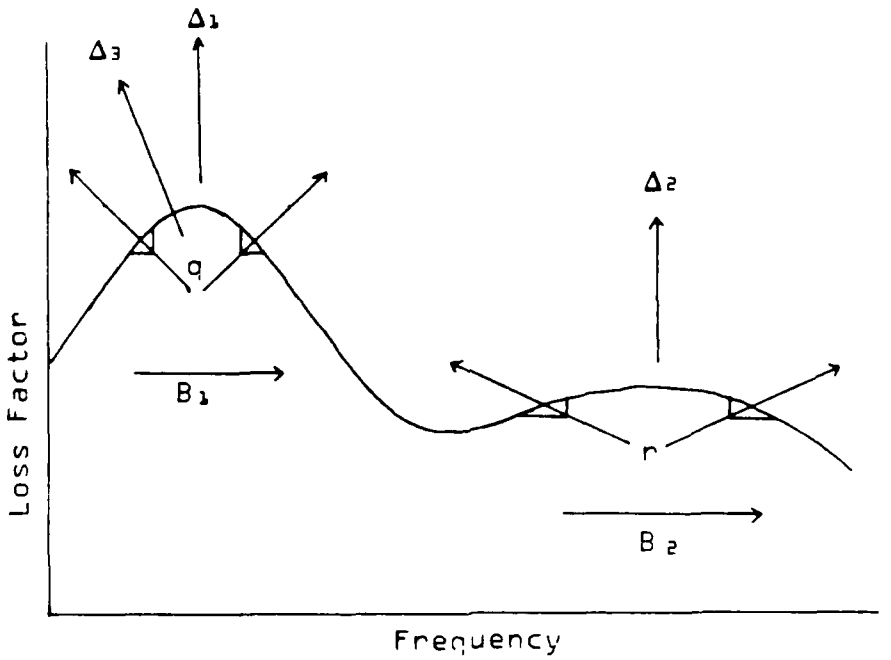

Figure 35. Effect of Parameter Variation on Two-ATF Model with Fractional Derivatives

V. Summary and Conclusions

In this study, the development of a model of material damping using augmenting thermodynamic fields (ATF), wherein the equations of thermodynamic equilibrium for these ATFs had derivatives of integer order, was reviewed. This model was originally introduced by Lesieutre, formerly of UCLA. The model was shown to be able to reproduce the material damping of classical thermoelastic and viscoelastic theory, with no assumptions made as to the magnitude of the the parameter Δ, given that E is taken to be the adiabatic modulus of elasticity for the thermoelastic case, or the glassy modulus for the viscoelastic case.

As an aside, if Δ is small as Lesieutre assumed, then the modulus of elasticity in the ATF model formulation, E, is approximately equal to the isothermal modulus of elasticity, E_T, of the thermoelastic model, or equal to E_o, the Young's modulus of the viscoelastic model.

The model of material damping was also developed wherein the thermodynamic equilibrium equations of the augmenting thermodynamic fields were allowed to have derivatives of fractional order. The ATF model with fractional derivatives was then compared to Bagley and Torvik's 4-parameter viscoelastic model, in which fractional derivatives are allowed as well. Comparison was a one to one match, given the fractions of each model's derivatives were equal. This comparison also showed that the Δ

parameter of the fractional order ATF model was less than unity. Moreover, in many materials Δ approached unity, i.e., $\Delta \geq 0.999$, since the glassy modulus for many materials is three orders of magnitude greater than the rubbery modulus. Owing to the fact that Bagley and Torvik have used the 4-parameter model to accurately model many materials over broad frequency ranges, assumptions that $\Delta << 1$, as Lesieutre made in his original model, cannot be made when using the ATF model to describe viscoelastic behavior in material damping.

The ATF model and the ATF model with fractional order derivatives, a more general case of the ATF model, was shown to lead to expressions for the loss factor and damping ratio that are strong functions of frequency, for the case of the uniaxial rod. This was the desired result. More importantly, the ATF model accurately describes actual behavior of many materials, because of the correspondence between it and the models of thermoelasticity and viscoelasticity.

In all comparisons, the modulus of elasticity, E, of the ATF model differed from the moduli of the respective models, E_T and E_o, by the factor $(1 - \Delta)$. In the case of viscoelasticity, the modulus E is found to be the glassy modulus, E_g, with the relationship between the rubbery modulus, E_o, and the glassy modulus being that of $E_o = (1 - \Delta)E_g$. A similar relation was shown to exist

between the isothermal and adiabatic moduli of the thermoelastic model, i.e., E_A, the adiabatic modulus of elasticity is related to E_T, the isothermal modulus of elasticity by the equation $E_A = (1 - \Delta)E_T$.

Recommendations for further study include examination of the linearity effects of this model. Determination of whether the sum of results obtained from a fractional order ATF modeling of viscoelasticity will describe material damping of materials in which both thermoelasticity and viscoelasticity are present need be made. It would appear to be so, since the fractional order ATF model is linear. This would also include experimental determination of the α_3 coupling parameter between strain and temperature.

It is recommended that the effects of higher order derivatives in the diffusion laws on the constitutive laws be determined. This will lead to an understanding of the exact relationship of the fractional order ATF model to thermoelasticity and viscoelasticity. The expansion of the model to three dimensions should present no particular difficulty.

Possible future research could also include an examination of energy methods as a means of deriving the ATF model.

Finally, it is recommended that numerical methods for the solution of the fractional order ATF model be ananlyzed. Application of numerical analysis to the fractional order

ATF model will allow for further ease in the use of the model in the description of material damping.

Appendix A:

Complex Numbers (Kreyszig, 1988:721-729)

Define a complex number, z, as

$$z = x + iy \tag{A.1}$$

where both x and y are real numbers, and

$$i^2 = -1 \tag{A.2}$$

is the definition of an "imaginary number."

The complex conjugate, z, of $\bar{z}$ is defined as

$$\bar{z} = x - iy \tag{A.3}$$

From these definitions, several relationships are developed:

$$Re\ z = x = 1/2(z + \bar{z}) \tag{A.4}$$

$$Im\ z = y = [1/(2i)](z - \bar{z}) \tag{A.5}$$

$$\left(\frac{\overline{z_1}}{z_2}\right) = \frac{\bar{z}_1}{\bar{z}_2} \tag{A.6}$$

The polar representation of the complex number z is often practical to use, and easier to manipulate mathematically. Define

$$x = r\cos(\theta)$$

$$y = r\cos(\theta) \tag{A.7}$$

By solving these equations simultaneously, it can be shown that

$$r = (x^2 + y^2)^{1/2}$$

$$\theta = \arctan(y/x) \tag{A.8}$$

Substituting equations (A.7) into equation (A.1) gives

$$z = r[\cos(\theta) + i\sin(\theta)] \tag{A.9}$$

It can also be shown mathematically that

$$z^n = r^n[\cos(n\theta) + i \sin(n\theta)] \qquad (A.10)$$

One of the most important complex analytical functions is the exponential function, defined as

$$e^z = e^x[\cos(y) + i \sin(y)] \qquad (A.11)$$

Substituting $z = iy$ into equation (A.11) gives the so-called *Euler Formula*:

$$e^{iy} = \cos(y) + i \sin(y) \qquad (A.12)$$

Comparing the right hand side of equation (A.9) to that of equation (A.12) gives

$$e^{i\theta} = \cos(\theta) + i \sin(\theta) \qquad (A.13)$$

and together with equation (A.9) gives the polar form of the exponential function:

$$z = r\, e^{i\theta} \qquad (A.14)$$

Solving equation (A.14) when $z = i$ gives

$$i = r[\cos(\theta) + i \sin(\theta)] \qquad (A.15)$$

For the equality of equation (A.15) to hold the following must be true:

$$r = (x^2 + y^2)^{1/2} = (0^2 + 1^2)^{1/2} = 1$$

$$\sin(\theta) = 1 \qquad (A.16)$$

Therefore,

$$\theta = (n\pi)/2, \quad n=1,2,3... \qquad (A.17)$$

So, recalling equation (A.13),

$$i = \cos(\pi/2) + i \sin(\pi/2) = e^{i(\pi/2)} \qquad (A.18)$$

for the principal value ($-\pi < \theta \leq \pi$).

For $z = (i)^f$ where $0 < f < 1$

$$z = i^f = (e^{i(\pi/2)})^f = e^{i(f\pi/2)} \quad \text{(A.19)}$$

From equations (A.10) and (A.18)

$$i^f = \cos(\theta) + i \sin(\theta) = \cos(f\pi/2) + i \sin(f\pi/2) \quad \text{(A.20)}$$

Appendix B:

Specific Heat Comparisons (Torvik, 1990)

Let the free energy of a solid undergoing a one-dimensional thermoelastic deformation be

$$F = E - TS \tag{B.1}$$

where

E = stored elastic energy
T = absolute temperature
S = entropy.

By the combined first and second laws of thermodynamics for this deformation

$$dE = TdS + \sigma d\epsilon \tag{B.2}$$

But

$$dF = dE - TdS - SdT \tag{B.3}$$

So

$$dF = \sigma d\epsilon - SdT \tag{B.4}$$

Thus

$$\partial F/\partial T\Big)_{\epsilon} = -S \tag{B.5}$$

and

$$\partial F/\partial \epsilon\Big)_{T} = \sigma \tag{B.6}$$

Hence it follows that

$$\partial S/\partial \epsilon\Big)_{T} = -\partial^2 F/(\partial\epsilon\partial T) = -\partial\sigma/\partial T\Big)_{\epsilon} \tag{B.7}$$

Recall that, for constant pressure,

$$c_p \Delta T = \Delta Q = T\Delta S \tag{B.8}$$

or

$$c_p = T\,\partial S/\partial T\Big)_{\sigma} \tag{B.9}$$

and, for constant volume (normal strain),

$$c_v \Delta T = \Delta Q = T \Delta S \tag{B.10}$$

or

$$c_v = T \left.\partial S / \partial T\right)_{\epsilon} \tag{B.11}$$

Now consider an incremental change in strain, at constant entropy:

$$d\sigma = \left.\partial \sigma / \partial \epsilon\right)_T \, d\epsilon + \left.\partial \sigma / \partial T\right)_{\epsilon} \, dT \tag{B.12}$$

So

$$\left.\partial \sigma / \partial \epsilon \right)_S = \left.\partial \sigma / \partial \epsilon\right)_T + \left.\partial T / \partial \epsilon\right)_S \left.\partial \sigma / \partial T\right)_{\epsilon} \tag{B.13}$$

Recall also that

$$\left.\partial x / \partial y\right)_z \left.\partial y / \partial z\right)_x \left.\partial z / \partial x\right)_y = -1 \tag{B.14}$$

Hence

$$\left.\partial T / \partial \epsilon\right)_S \left.\partial \epsilon / \partial S \right)_T \left.\partial S / \partial T\right)_{\epsilon} = -1 \tag{B.15}$$

So

$$\left.\partial T / \partial \epsilon\right)_S = - \left.\partial S / \partial \epsilon\right)_T \left.\partial T / \partial S\right)_{\epsilon} \tag{B.16}$$

Also,

$$\left.\partial \sigma / \partial \epsilon\right)_T \left.\partial \epsilon / \partial T\right)_{\sigma} \left.\partial T / \partial \sigma \right)_{\epsilon} = -1 \tag{B.17}$$

So

$$\left.\partial \sigma / \partial T\right)_{\epsilon} = - \left.\partial \sigma / \partial \epsilon\right)_T \left.\partial \epsilon / \partial T\right)_{\sigma} \tag{B.18}$$

Substituting equation (B.16) into equation (B.13), then using equations (B.7), (B.8) and (B.11) we find

$$\left.\partial \sigma / \partial \epsilon\right)_S = \left.\partial \sigma / \partial \epsilon\right)_T + \left[\left.\partial \epsilon / \partial \sigma\right)_T\right]^2 \left[\left.\partial T / \partial \epsilon\right)\right]^2_{\sigma} \, T / c_v \tag{B.19}$$

or

$$\left.\partial \sigma / \partial \epsilon\right)_S = \left.\partial \sigma / \partial \epsilon\right)_T + \left[\left.\partial \sigma / \partial \epsilon\right)_T\right]^2 \left[\left.\partial \epsilon / \partial T\right)_{\sigma}\right]^2 \, T / c_v \tag{B.20}$$

or

$$E_A = E_T + E_T^2 \alpha^2 T / c_v \tag{B.21}$$

where

E_A is the adiabatic Young's modulus,
E_T is the isothermal modulus, and
α is the linear coefficient of thermal expansion.

Thus,

$$E_A = E_T[1 + (E_T\alpha^2 T)/c_v] \qquad (B.22)$$

Note that c_v here is the energy change, per unit volume, for a unit temperature change.

Bibliography

BAGLEY, Ronald L. Applications of Generalized Derivatives to Viscoelasticity. PhD dissertation. School of Engineering, Air Force Institute of Technology (AU), Wright-Patterson AFB, November 1979.

BAGLEY, Ronald L. and TORVIK, Peter J. "On the Fractional Calculus Model of Viscoelastic Behavior," Journal of Rheology, 30(1): 133-155 (1986).

BAGLEY, Ronald L. and TORVIK, Peter J. "Fractional Calculus - A Different Approach to the Analysis of Viscoelastically Damped Structures," AIAA Journal, 21: 741-748 (May 1983).

BOLEY, Bruno A. and WEINER, Jerome H. Theory of Thermal Stresses. New York: John Wiley & Sons, Inc. 1960.

CALLEN, Herbert B. Thermodynamics. New York: John Wiley & Sons, 1960.

CAPUTO, M. "Vibrations of an Infinite Plate with a Frequency Independent Q," Journal of the Acoustical Society of America, Vol. 60: 634-637 (1976).

CHRISTENSEN, R. M. Theory of Viscoelasticity, An Introduction (Second Edition). New York: Academic Press, 1971.

KOVALENKO, A. D. Thermoelasticity: Basic Theory and Applications. Translated from the Russian by D. Maeven, Groningen: Volters-Noordhoff Publishing, 1969.

KREYSZIG, Erwin. Advanced Engineering Mathematics. New York: John Wiley and Sons, 1988.

LESIEUTRE, George A. Finite Element Modeling of Frequency-Dependent Material Damping using Augmenting Thermodynamic Fields. PhD dissertation. Aerospace Engineering, University of California, Los Angeles CA, 1989.

MEIROVITCH, Leonard. Analytical Methods in Vibrations. New York: Macmillan Publishing Co., Inc., 1967.

MEIROVITCH, Leonard. Elements of Vibration Analysis. New York: McGraw-Hill Book Company, 1986.

NOWICK, A. S. and BERRY, B. S. Anelastic Relaxation in Crystalline Solids. New York: Academic Press, 1972.

OLDHAM, Keith B. and SPANIER, Joseph The Fractional Calculus. New York: Academic Press, 1974.

PENNER, S. S. Thermodynamics for Scientists and Engineers. Reading: Addison-Wesley Publishing Company, 1968.

SPANNER, D. C. Introduction to Thermodynamics. New York: Academic Press, 1964.

TORVIK, Peter J. "Damping of Layered Materials." Address to the 30th Structures, Structural Dynamics and Materials Conference. AIAA Paper #89-1422 (1989).

TORVIK, Peter J., Derivation provided from personal notes. Department of Aeronautics and Astronautics, Air Force Institute of Technology (AU), Wright Patterson AFB, 4 September 1990.

TORVIK, Peter J. and BAGLEY, Ronald L. "Fractional Derivatives in the Description of Damping Materials and Phenomena," The Role of Damping in Vibration and Noise Control, Edited by L. Rogers and J. Simonis, ASME, 125-136 (1987).

TORVIK, Peter J. and BAGLEY, Ronald L. "On the Appearance of the Fractional Derivative in the Behavior of Real Materials," Journal of Applied Mechanics, 51: 295-299, (June 1984).

ZENER, Clarence M. Elasticity and Anelasticity of Metals. Chicago: The University of Chicago Press, 1948.

Vita

First Lieutenant David S. [redacted] He graduated with honors from high school in Woods Cross, Utah, in 1979. Following graduation, he served for two years as a religious missionary in Brazil. Starting in 1982, he attended the University of Utah, from which he graduated Cum Laude with the degree of Bachelor of Science in Mechanical Engineering in December 1986. As a Distinguished Graduate, he received his commision in the USAF from Officer Training School in March of 1987, following which he was assigned to Wright-Patterson Air Force Base in Dayton, Ohio, where he worked as a Vibration and Loads Engineer for the Deputy of Engineering, Aeronautical Systems Division. In June of 1988 he was collocated to the Advanced Cruise Missile System Program Office, where he filled the Lead Structures Engineer slot, until entering the School of Engineering, Air Force Institue of Technology, in May 1989.

Lt. Hansen is married to the former Lisa Merrill of Bountiful, Utah. They have three children: Nathan, who is six; Ryan, a handful at two years, and Megan, the sweetheart of their lives at one.

[redacted]

REPORT DOCUMENTATION PAGE

Form Approved
OMB No. 0704-0188

1. AGENCY USE ONLY *(Leave blank)*	2. REPORT DATE	3. REPORT TYPE AND DATES COVERED
	1990 September	MS Thesis

4. TITLE AND SUBTITLE
FREQUENCY-DEPENDENT MATERIAL DAMPING USING AUGMENTING THERMODYNAMIC FIELDS (ATF) WITH FRACTIONAL TIME DERIVATIVES

5. FUNDING NUMBERS

6. AUTHOR(S)
David S. Hansen, B.S., 1st Lt, USAF

7. PERFORMING ORGANIZATION NAME(S) AND ADDRESS(ES)
School of Engineering
AFIT/ENY
Air Force Institute of Technology (AU)
Wright-Patterson AFB, Ohio 45433-6583

8. PERFORMING ORGANIZATION REPORT NUMBER
AFIT/GAE/ENY/90S-1

9. SPONSORING / MONITORING AGENCY NAME(S) AND ADDRESS(ES)

10. SPONSORING / MONITORING AGENCY REPORT NUMBER

11. SUPPLEMENTARY NOTES

12a. DISTRIBUTION / AVAILABILITY STATEMENT
Approved for public release;
Distribution unlimited

12b. DISTRIBUTION CODE

13. ABSTRACT *(Maximum 200 words)*

Thesis Advisor: Peter J. Torvik
Professor
Department of Aeronautics and Astronautics

14. SUBJECT TERMS
Augmenting Thermodynamic Fields
Fractional Derivatives
Material Damping
Thermoelastic Damping
Viscoelastic Damping

15. NUMBER OF PAGES
103

16. PRICE CODE

17. SECURITY CLASSIFICATION OF REPORT	18. SECURITY CLASSIFICATION OF THIS PAGE	19. SECURITY CLASSIFICATION OF ABSTRACT	20. LIMITATION OF ABSTRACT
Unclassified	Unclassified	Unclassified	

ABSTRACT

This study developed a material damping model using the concept of augmenting thermodynamic fields (ATF), wherein the equations of thermodynamic equilibrium are allowed to have derivatives of fractional order. This effort seeks to expand the applicability of the ATF model of Lesieutre, formerly of UCLA, in which ATFs interact with the mechanical displacement fields.

Current models of material damping cannot predict well the dependency of damping on frequency. Two newer models, capable of predicting this frequency dependence, are discussed. They include the ATF model, and Bagley and Torvik's, AFIT, 4-parameter model, which allows fractional derivatives in the description of viscoelastic materials.

This research effort applies fractional-order derivatives to the ATF model. Coupled material constitutive relations are developed using the concept of augmenting thermodynamic fields, with non-integer differentials allowed in the resulting partial differential equations.

The complex modulus that results from solution of these partial differential equations is compared to the complex moduli of thermoelasticity, integer-order viscoelasticity, and viscoelasticity with fractional derivatives (the 4-parameter model) for the case of a uniaxial rod. In each case, the fractional-order ATF model reduced to the respective model, and therefore, accurately describes the damping mechanism resulting from each of these models.